UNIVERSITY OF GAZİANTEP
GRADUATE SCHOOL OF
NATURAL & APPLIED SCIENCES

FINITE ELEMENT MODELING AND ANALYSIS OF REINFORCED CONCRETE BEAMS WITH STEEL FIBER AND STEEL PLATE

M.Sc. THESIS
IN
CIVIL ENGINEERING

BY
HEBA KADHM AL-AZZAWI

JUNE 2015

Finite Element Modeling and Analysis of Reinforced Concrete Beams with Steel Fiber and Steel Plate

M.Sc. Thesis

in

Civil Engineering

University of Gaziantep

Supervisor:

Assoc. Prof. Dr. Esra METE GÜNEYİSİ

by

Heba Kadhm AL-AZZAWI

June 2015

REPUBLIC OF TURKEY
UNIVERSITY OF GAZİANTEP
GRADUATE SCHOOL OF NATURAL & APPLIED SCIENCES
CIVIL ENGINEERING

Name of the thesis: Finite element modeling and analysis of reinforced concrete beams with steel fiber and steel plate

Name of the student: Heba Kadhm AL-AZZAWI

Exam date: June, 4, 2015

Approval of the Graduate School of Natural and Applied Sciences.

Prof. Dr. Metin BEDİR

Director

I certify that this thesis satisfies all the requirements as a thesis for the degree of Master of Science.

Prof. Dr. Mustafa GÜNAL

Head of Department

This is to certify that we have read this thesis and that in our consensus/majority opinion it is fully adequate, in scope and quality, as a thesis for the degree of Master of Science.

Assoc. Prof. Dr. Esra METE GÜNEYİSİ

Supervisor

Examining Committee Members	Signature
Assoc. Prof. Dr. Esra METE GÜNEYİSİ	....
Assoc. Prof. Dr. Mehmet GESOĞLU	....
Assist. Prof. Dr. Kasım MERMERDAŞ	....

I hereby declare that all information in this document has been obtained and presented in accordance with academic rules and ethical conduct. I also declare that, as required by these rules and conduct, I have fully cited and referenced all material and results that are not original to this work.

Heba Kadhm AL-AZZAWI

ABSTRACT

FINITE ELEMENT MODELING AND ANALYSIS OF REINFORCED CONCRETE BEAMS WITH STEEL FIBER AND STEEL PLATE

AL-AZZAWI, Heba Kadhm

M.Sc. in Civil Engineering

Supervisors: Assoc. Prof. Dr. Esra METE GÜNEYİSİ

June 2015, Pages 88

In this study, a numerical analysis was carried out by using ANSYS finite element software to model and evaluate the structural behavior of full-size reinforced concrete (RC) beams having different properties. For this, a reference beam having a span length of 6.5 m was designed. Then, two cases were considered to enhance the structural performance of the RC beam. In the first case, the use of steel fiber in RC beam was taken account. Three steel fiber volume fractions (0.5, 1.0, and 2.0%) were investigated. In the second case, the bonding of steel plate to the tension face of the beam by adhesive resin was considered. Various thicknesses of steel plate (1, 2, and 3 mm) was utilized in this case. All beams were subjected to a three-point bending test. The nonlinear property was modeled for the concrete using three-dimensional (3D) solid element. The steel reinforcing bars were modeled as linkage elements with elasto-plastic behavior and perfect bond between concrete element and steel bar was assumed. The steel plate used for strengthening RC beam was modeled as a plane shell element connected to the lower concrete surface by using special contact surface between them. The steel fibers were considered as small units of reinforcement embedded in concrete based on the geometry of the concrete element. The efficiency of the current models was measured by comparing the results with previous experimental results. A good agreement was found between the model predictions for the load-deflection relation and experimental results. Besides, the use of steel plate for strengthening conventional RC beam significantly increased the ultimate load carrying capacity as well as the stiffness of the beam more than that of the steel fiber cases, especially when a steel plate thickness was chosen as 3 mm.

Keywords: Finite element method, Reinforced concrete beam, Steel fiber, Steel plate, Strengthening.

ÖZET

ÇELİK LİFLİ VE ÇELİK PLAKALI BETONARME KİRİŞLERİN SONLU ELEMANLAR YÖNTEMİ İLE MODELLENMESİ VE ANALİZİ

AL-AZZAWI, Heba Kadhm

Yuksek Lisans, İnşaat Mühendisliği Bölümü

Danışman: Doç. Dr. Esra METE GÜNEYİSİ

Haziran 2015, Sayfa 88

Bu çalışmada, ANSYS sonlu elemanlar programı kullanılarak farklı özelliklere sahip gerçek boyuttaki betonarme kirişlerin yapısal davranışlarını modellemek ve değerlendirmek için nümerik bir analiz yapılmıştır. Bunun için, öncelikle 6.5 m açıklığında referans bir kiriş tasarlanmıştır. Daha sonra, betonarme kirişin yapısal performansını iyileştirmek için iki durum düşünülmüştür. İlk durumda, betonarme kirişlerde çelik lif kullanımı dikkate alınmıştır. Üç farklı hacimsel oranında (%0.5, %1.0 ve %2.0) çelik lif etkisi incelenmiştir. İkinci durumda ise, kirişin çekme yüzeyine epoksi ile çelik plaka yapıştırılarak güçlendirilmesi göz önünde bulundurulmuştur. Çeşitli kalınlıktaki çelik plakalar (1, 2 ve 3 mm) bu durumda kullanılmıştır. Bütün kirişler üç noktalı eğilme deneyine tabii tutulmuştur. Betonun lineer olmayan davranışının modellenmesinde üç boyutlu (3D) katı eleman kullanılmıştır. Çelik donatı çubukları elasto-plastik davranışlı bağlantı elemanları olarak modellenirken, beton ile çelik arasında mükemmel bağ olduğu varsayılmıştır. Betonarme kirişi güçlendirmek için kullanılan çelik plaka, aralarında özel bağlantı yüzeyi kullanılarak kirişin alt yüzeyine bağlanan düz kabuk eleman olarak modellenmiştir. Çelik lifler, beton elemanının geometrisine bağlı olarak beton içinde saklı küçük güçlendirme birimleri olarak düşünülmüştür. Araştırmada, mevcut modellerin verimliliği önceki deneysel sonuçlarla kıyaslanarak ölçülmüştür.Yük-deplasman ilişkisini tahmin eden model ile deneysel sonuçlar arasında iyi bir uyumun olduğunu araştırma sonuçları göstermiştir. Ayrıca, geleneksel betonarme kirişi güçlendirmek için kullanılan çelik plaka özellikle çelik plaka kalınlığı 3 mm olarak seçildiğinde, nihai yük taşıma kapasitesini ve betonarme kirişlerin rijitliğini çelik lif kullanılan durumlardan daha fazla artırmıştır.

Anahtar kelimeler: Sonlu elemanlar yöntemi, Betonarme kiriş, Çelik lif, Çelik plaka, Güçlendirme.

ACKNOWLEDGEMENTS

First of all, great thanks to Allah his Majesty for enabling me to complete this work.

I would like to express my respect and regards to my supervisor, Assoc. Prof. Dr Esra Mete Güneyisi for her guidance, advice, encouragement and suggestions during the preparation of this thesis.

This thesis is a milestone in my academic career. I have been fortunate learn theories and concepts which would have been impossible if I had not extensively carried out the needed research. I am grateful to a number of people who have guided and supported me throughout the research process and provided assistance for my venture.

All my words cannot express about my thanks to my husband for his interest during this thesis Hesham Abd Latef Numan.

My special thanks are reserved for my family and my kids for their understanding, patience and great help.

Finally, I dedicate my efforts to my mother's spirit (God's mercy on her).

TABLE OF CONTENTS

LIST OF FIGURES

Page

LIST OF TABLES

Page

LIST OF ABBREVIATIONS

RC	Reinforced Concrete
3D	Three dimensional
FRC	Fiber Reinforced Concrete
SF	Steel Fiber
SP	Steel Plate
FEM	Finite Element Method
ACI	American concrete institute
SFRC	Steel Fiber Reinforced Concrete
ts	Thickness of steel plate
tg	Thickness of glue
EX	Modulus of Elasticity
PRXY	Poisson’s ratio
fy	Yield stress
Et	Tangent modulus
RB	Reinforced concrete beam without any strengthening
RB-SF0.5	Reinforced concrete beam with strengthening 0.5% steel fiber
RB-SF1.0	Reinforced concrete beam with strengthening 1.0% steel fiber
RB-SF2.0	Reinforced concrete beam with strengthening 2.0% steel fiber

RB-SP1	Reinforced concrete beam with strengthening of 1 mm of steel plate
RB-SP2	Reinforced concrete beam with strengthening of 2 mm of steel plate
RB-SP3	Reinforced concrete beam with strengthening of 3 mm of steel plate

CHAPTER 1

INTRODUCTION

1.1 General

Some of the undesirable characteristics of the concrete as a brittle material is its low tensile strength about 10% to 15%, and shear strength is about 35% to 80% of its compressive strength. Thus, it requires reinforcement so as to utilize as the most widely construction material as well known reinforced concrete (RC). Traditionally, this reinforcement is in the modality of continuous steel bars placed in the concrete structure in suitable positions to resist the imposed tensile and shear stresses. The existence of fibers, on the other hands, is generally discontinuous, short, and randomly distributed throughout the concrete member to make a composite structure material known as fiber reinforced concrete (FRC) (Jyoti et al., 2013).

Fibers are mostly made of steel, glass, and polymer or fabricated from natural materials. The existence of fibers in concrete can reduce crack propagation effectively because of their tendency to be more closely spaced than traditional reinforcing steel bars. However, they are not considered as an alternative material for traditional steel bars since they have different functions to play in advanced concrete technology (Ganesan and Indira, 2000; Rana, 2013).

Steel fiber (SF) is widespread kind of fiber utilized as concrete reinforcement. The major factors affecting the behavior of RC, with SF are: volume and distribution of SF in section, anchorage of SF in concrete matrix, yield strength of SF and strength of concrete (Remigijus and Gediminas, 2007).

The previous studies indicated that the SF added RC structures had higher shear strength, flexural toughness, impact resistance, ductility, and lower crack propagation and crack widening (Gambhir, 1995; Altun et al., 2006). Therefore, it has been applied in many importance jobs of construction, tunnel linings, shell domes, dam construction, seismic retrofit, spillways, airport runways, and highway pavements (Vikrant et al., 2012).

On the other hand, to produce a structural member with high load carrying or to enhance the capacity of such member, the useful properties of various materials can be connected. Then, the structural member of two or more materials is well known a composite member. For example, the strengthening RC beam by steel plate (SP) at the lower face is one approach of the composite beam. Ideally, the connection between steel plate and concrete member is a partial interaction phenomenon due to comparatively flexible material utilized that connect between them weather anchor bolts or glue or together (Jones et al., 1980).

Finite Element Method (FEM) utilizes a powerful and general analytical tool to evaluate the performance of the structures. Cracking, linear or non-linear material properties, interface between elements, and other effects treated in very accurate results can be modeled worthily compared with other numerical methods. It is worth to mentioning, that simple analytical methods are not capability for the solution of intricate civil engineering problems, and the FEM offers an effective, versatile, and reliable way to handle such cases. One of the most important programs used in the FEM is ANSYS program (Lihua et al., 2008).

In some conventional RC constructions, the structures are subjected to increasingly service load conditions. Therefore, in recent years, the maintenance, repair, and strengthening of such structures are significantly increased. Moreover, the RC components gradually lose their ability to support or carry the increasing of load with time and deterioration due to fatigue, creep factors, and corrosion.

Reinforcing existing RC beam by bonding steel plate (SP) at the lower face by adhesive resin is very important method to obtain more resistance for increasing loading. On the other hand, in the newly constructed RC beams, the use of steel fiber (SF) can be considered as a remedy to enhance the capacity of the beams in terms of strength and ductility or to limit the possibility of crack prorogation.

1.2 Objective and Scope

In this study, FEM models were developed to evaluate the behavior of three-dimensional (3D) full-size RC beams having different properties through nonlinear response until approached a failure load by using ANSYS program (SAS, 2005). For this, firstly, a reference RC beam was designed. Then, two different cases were considered to improve the flexural performance of the RC beam. In the first case, the addition of steel fibers to RC beam was taken account. Three steel fiber-volume fractions (0.5, 1.0, and 2.0 %) were investigated, while in the second case, the bonding of steel plate to the tension face of the beam by adhesive resin was considered. Different thickness of steel plate (1, 2 and 3 mm) was used in this case. Comparison was established on the results between two strategies, which were deflection, ductility in addition to crack pattern and mode of failure and decided which strategy is the best to be used for enhancing the structural response of the conventional RC beam.

1.3 Outline of the thesis

This thesis is divided into five chapters. Current chapter provides evidence of the need to study the effects of strengthening reinforced concrete beam.

Background and summarizes of previous research, which have been conducted on steel fibers and steel plate for reinforcing concrete beam, are presented in Chapter 2.

Chapter 3 presents the 3D analysis by ANSYS program, which is common in most publications about strengthening the concrete beam by the straight steel fiber through the beam for different volume of fraction and steel plate at the lower tension face with different thicknesses.

In Chapter 4 contains the result and discussions, in addition to, verified the current models with experimental results data in previous studies.

In Chapter 5 includes the conclusions and comparison between the two strategies of strengthening the reinforced concrete beam.

CHAPTER 2

LITERATURE REVIEW AND BACKGROUND

The characteristics of each material vary from the characteristics of another material; therefore there is no material that can satisfy all the structural demands. This is the reason of using two or more materials and connecting them together in order to make full advantage of their properties in getting one structural component that uses the eligible characteristics of the materials. In structural retrofitting field, the maintenance, repair and upgrading o RC structures are just as an important and technical points as the design and construction of the modern structures. Additional steel fibers and steel plate are now identified as an effective way to enhance the strength and ductility of conventional RC structures due to these superior properties (Madana et al., 2007; Hesham, 2010).

2.1 Steel fiber applications

Historically, from a long time ago, seemed to need for raising tensile strength of concrete started in 1874, Bernard was the first suggested to strength concrete by adding steel fragments. After 36 years from that date Porter preceded the possibility of adding short wire (nails) to concrete. After that, in 1918, Alfsen patented a way of upgrading concrete by long steel fibers (SFs), long wooden fibers, and fibers made of natural material based on him, the addition of like fibers was responsibility to increase tensile strength of concrete (Maidl ,1995) . However the existence of any type of fiber to reinforce concrete can be defined as a composite material containing of hydraulic cements consisting fine or coarse and fine aggregate and discontinuous separate fibers (ACI 544.1, 1996).

2.1.1 Classification and type of SFs

There are a various kinds of SFs which are classified according to shape and production process. Round, straight steel fibers are manufactured with wire. Precipitant wires diameter ranging from 0.25 to 1.00 mm and lengths from 7.0 to75 mm, this sort of fibers are result from cutting the wire into small pieces. Flat, straight steel fibers ordinarily have cross sections worth from 0.25 to 2.03 mm width by 0.15 to 0.64 mm thickness is shaped by shearing sheet or devastation wire. Folded SFs have been formed with whoever full length folding, or enlarged at the end (Kamran, 2012).

Bending fibers or flattering fibers have been done for increasing mechanical bonding. The SFs are designed specifically for strengthening of concrete and cementitous mixes. These are cold drawn wire fiber and they are distorted with hooked end to progress most appropriate anchorage within the concrete mix (ACI 544.1, 1996; Xu et al., 2011), as shown in Figure 2.1.

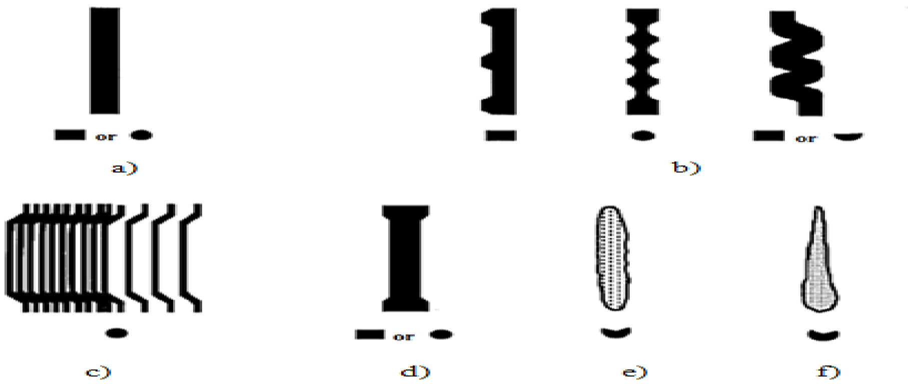

Figure 2.1 Shape of steel fibers: a) straight slit sheet or wire, b) deformed slit sheet or wire, c) crimped-end wire, d) flattened-end slit sheet or wire, e) machined chip, and f) melt extract (ACI 544.1, 1996)

Banthia and Trottier (1994) studied the pullout behavior of hooked, crimped, and stranded SFs embedded in concrete matrices with various strengths. In concrete matrices were used aggregates with a maximum size 3/8 inches (10 mm). The fibers were tilted from the loading orientation at an angle that changed from 0 to 90 degrees. Only test results for hooked SFs with 0-degree tendency are listed in Table 2.1. They found that joint strength improved with respect to an increase in matrix strength.

However, relative to the results for a cement-based matrix, an increase in the concrete matrix strength led to only humble increase in the average joint stress at failure load. Moreover, the slips at failure load were greater when a concrete matrix was utilized.

Table 2.1 Test results related to hooked steel fibers embedded in a concrete matrix (Banthia and Trottier, 1994)

Diameter (in.)	Embedded length (in.)	Matrix strength (psi)	Failure load (lb)	Deflection at failure load (in.)	Average bond stress at failure load (psi)
0.0295	1.18	5800	61	0.061	560
		7540	65	0.039	590
		12330	67	0.047	610

The load-slip behavior of the concrete having different strengths was also discussed in the study of Banthia and Trottier (1994). Figure 2.2 illustrates the influence of fiber inclination angle with respect to the loading orientations for normal-strength, mid-strength, and high-strength concrete (5.8, 7.5, and 12.3 ksi, respectively). Normal-strength and mid-strength of concrete, a change in the angle from 0 to 15 degrees did not noticeably affect the load-slip curve. When the orientation angle increased after 30 degrees, the influence of fiber inclination was more pronounced up to a slip of 0.14 in. (3.5 mm).

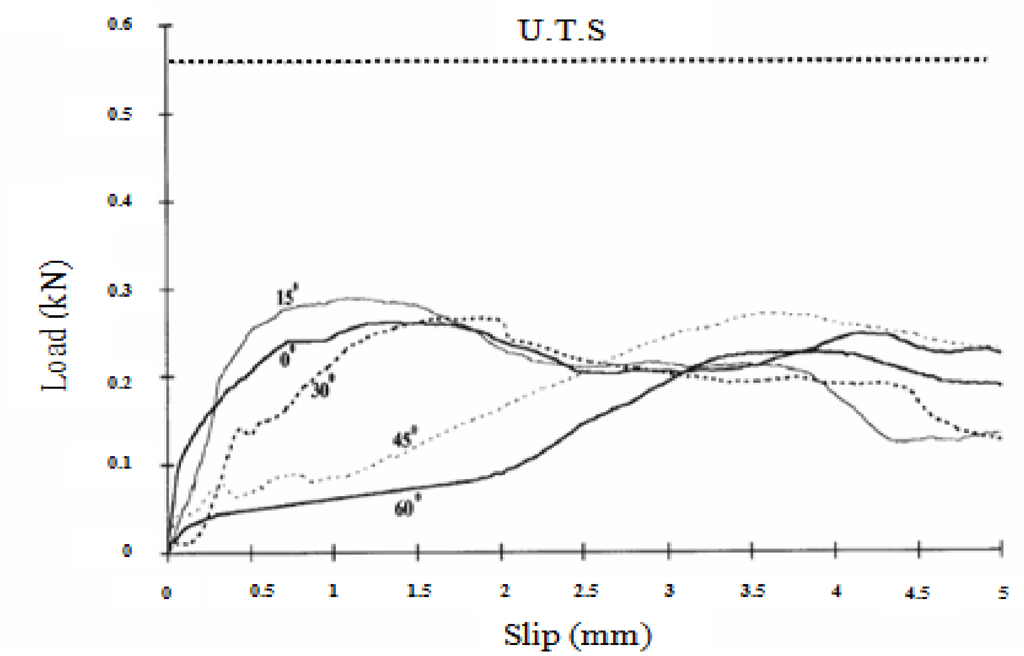

a)

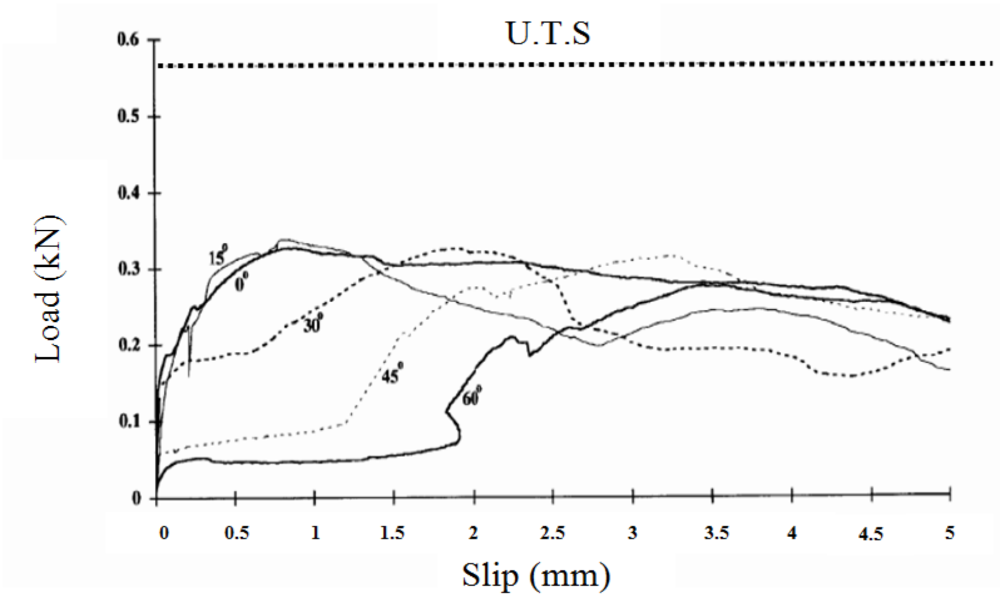

b)

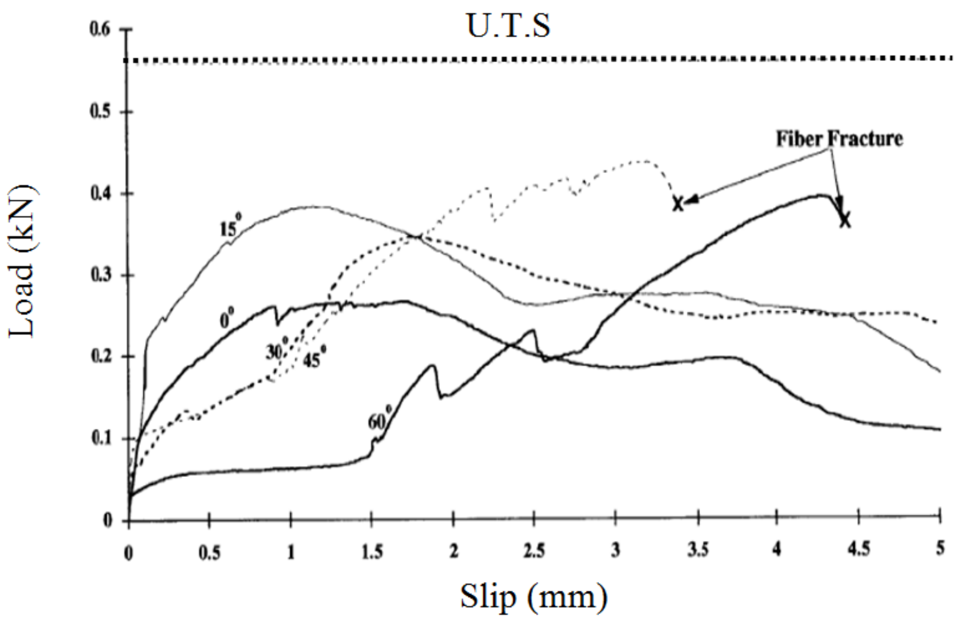

c)

Figure 2.2 Effect of fiber orientation for hooked steel fiber in a) normal- strength, b) mid- strength, and c) high strength of concrete (Banthia and Trottier, 1994)

2.1.2 Physical Properties of SFs

The performance RC structures greatly based on characteristics bond between SF and concrete, therefore, the development of various types of SFs has been driven to improve these characteristic. However, the essential source of bond for these fibers comes from the friction forces between the SFs and concrete. Therefore, SFs with a smaller surface area to volume ratio have smaller bond strengths. Hence, the SFs with circular sections are less activity than fibers with rectangular sections for the same fiber length. A SF has a diameter that is much smaller than its length. The length to equivalent diameter (L/D) ratio is called as the aspect ratio. Generally, aspect ratios range from 20 to 100. Continuous SFs have long aspect ratios; while discrete SFs have short aspect ratios fibers with larger lengths (higher aspect ratio) were more activity (Zollo, 1996).

The fibers produce high-strength due to their small diameter; they contain far fewer flaws (normally surface flaws) compared to the material generated in bulk. As a general method, the smaller the diameter of the fibers, the higher its strength, but oftentimes the addition cost as the diameter becomes smaller. Besides that, smaller-diameter high-strength steel fibers have greater elasticity and are more adjustable to manufacturing processes such as knitting or shaping over radii (Campbell, 2010).

In recent years, many studies have been conducted to optimize the form and size of SFs to achieve enhanced fiber- matrix bond properties and improved fiber dispensability. It was found that SFs with hook-ended stainless steel wires had better physical characteristics than those straight fibers due to the increment in the effective aspect ratio (Nataraja et al, 1999).

Mahendra et al. (2010) presented an experimental study of using the proportion of SFs with artificial sand as a fine aggregate in concrete matrices. The SFs were crimpled and volume fraction ranging from 0 to 2.0% at an interval of 0.5% by volume of concrete specimens .They observed the shape of the particles in artificial sand was very important factor on the bond strength, thus increased compressive strength, flexural strength, and split tensile strength, respectively. Beside that they were found the optimum volume fraction for steel fiber was 1.5% with superplasticizer and significantly reduced a bleeding from concrete when used artificial sand.

Jyoti et al. (2013) used thirteen specimens of concrete specimens in their experimental work by addition a different volume fraction of SFs (0.5%, 1.0%, 1.5% and 2.0%, respectively) and used different aspect ratio. They found that the existence of SFs into concrete mixture played an important role which it was increased the rotation capacity of beam-column joint at the ultimate load as compared to without existence steel fibers in these joints.

Wasan and Tayfur (2013) conducted an experimental work on eleven ultra-high performance RC beam specimens reinforced by SFs to investigate the effect of flexural behavior of RC beams. Different of volume fraction of steel fibers from 0.5 to 1.0% were conducted which they added at different levels of the depth of RC beam specimens.

Moreover, different types of steel fibers used in their work. It was noted as the increasing noticeable the flexibility and toughness, in addition, the inconspicuous effect on load-deflection behavior, ultimate moment capacity, and cracking pattern for any type of steel fibers.

2.1.3 Dynamic strength of SFs

Naaman and Najm (1991) observed that an increase in matrix strength led to an increase in attached strength and a faster debonding. Pulling out a hooked steel fiber needed a work that was four times greater than that needed for a smooth steel fiber. The slip at failure load when pulling out a smooth SF was up to two times smaller than that for a hooked SF. Test results relevant to hooked SFs are showed in Table 2.2. It can be observed that the slips at failure loads were less than 0.04 inches (1 mm) and the average bond stress changed from 640 to 1110 psi, according to matrix strength.

Table 2.2 Pullout test results pertinent to hooked steel fibers embedded in a cement-based matrix (Naaman and Najm, 1991)

Diameter (in.)	Embedded length (in.)	Matrix strength (psi)	Failure load (lb)	Deflection at failure load (in.)	Average bond stress at failure load (psi)
0.0295	1	4850	59	0.031	640
		7400	80	0.035	860
		8650	103	0.029	1110

Figure 2.3 illustrates the influence of embedment length and matrix strength. Doubling the embedment length of the fibers did not noticeably affect the load-slip curves due to the hooked ends participated most of the effective attach strength of the fibers (Naaman and Najm, 1991).

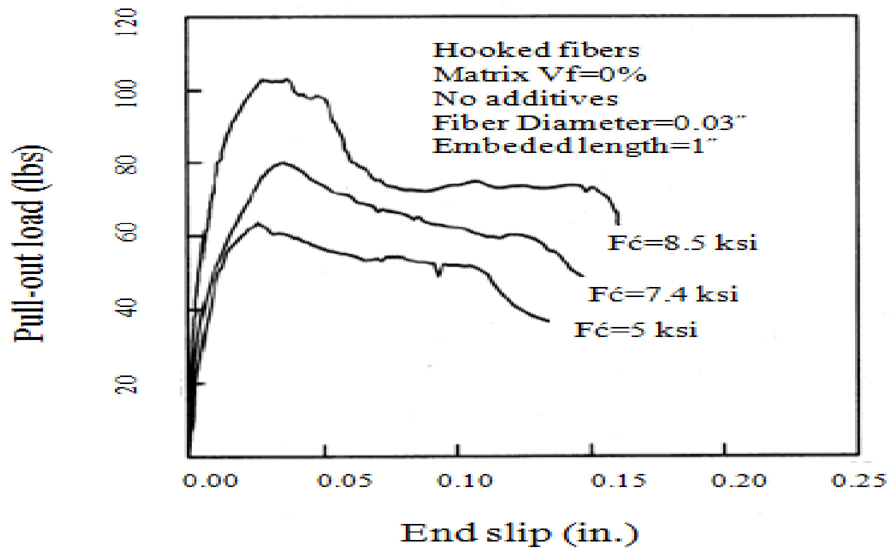

a)

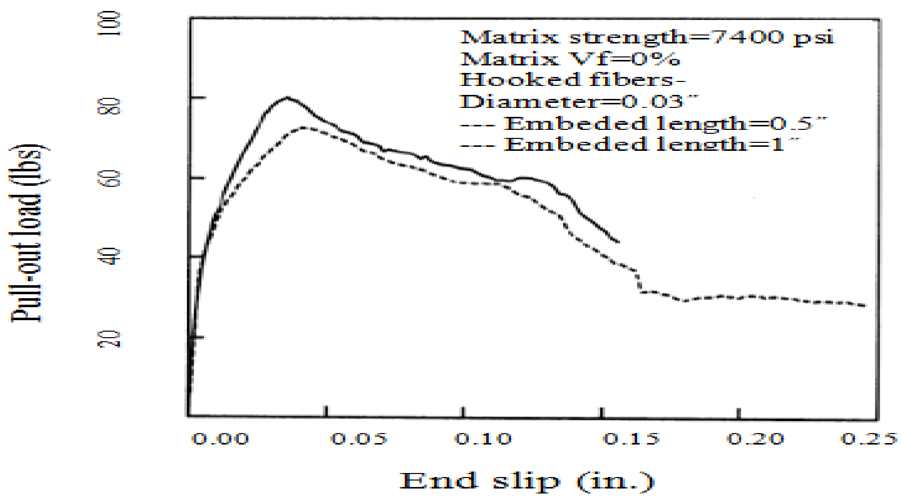

b)

Figure 2.3 Effect of a) matrix strength and b) fiber embedment length on pullout behavior (Naaman and Najm, 1991)

2.1.4 Effect of SF on workability

Slump experiments were conducted to examine the workability and consistency of fresh concrete. The eligibility of SF reinforcement is dependent upon accomplishment of a regular distribution of the SF in the concrete, their interaction with the cement matrix, and the capability of the concrete to be successfully mold or sprinkled (Brown and Atkinson, 2012).

Basically, each component of the SFs needs to be coated with cement paste to supply any benefit in the concrete. Regular use of SFs to reinforce the concrete can be obtained byt adding more fibers into the concrete, particularly of a very small diameter product in a greater negative influence on the workability and the exigency for the mix design changes as shown in Figure 2.4 (Endgington, 1974). The slump can be affected different kind of fiber content and shape.

The reason of lower slump is that inserting steel fibers can form a grid structure in concrete, which curb mixture from secession and flux. By virtue of the high content and large superficies area of SFs, these fibers are sure to suck more cement paste to wrap around and the addition of the stickiness of mixture induces the slump loss (Chen and Liu, 2000).

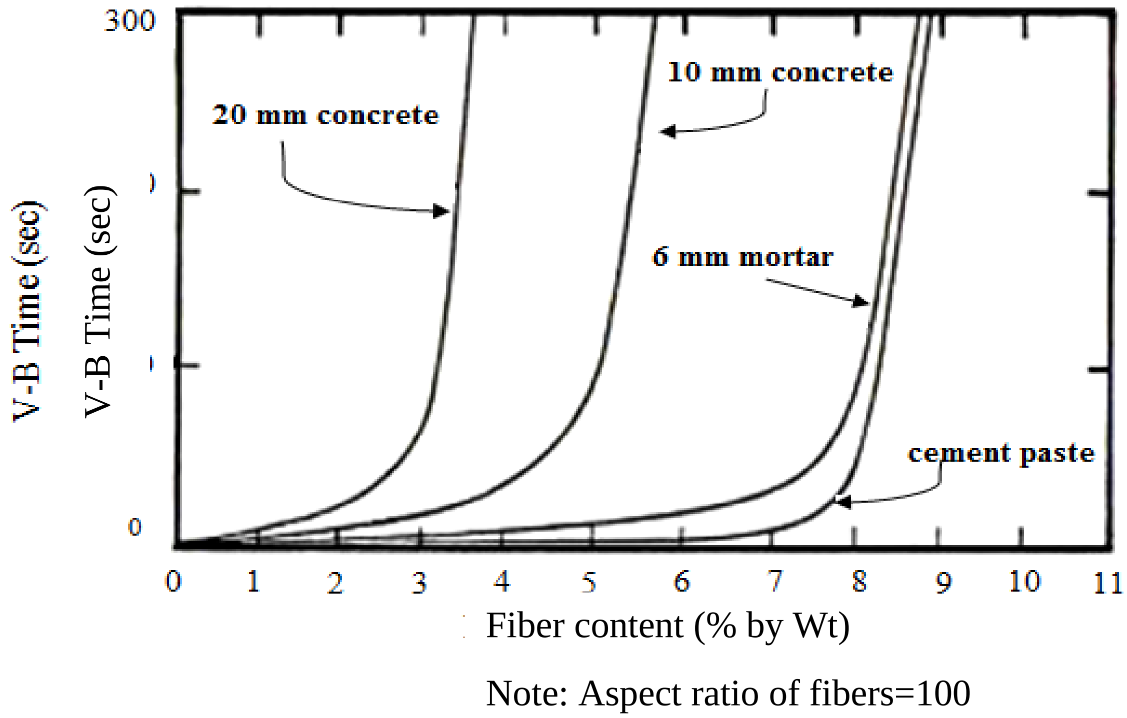

Figure 2.4 Workability versus fiber content for matrices with different maximum aggregate sizes (Endgington, 1974)

Corresponding to many researchers, the addition of SFs throughout concrete makes low workable or inadequate workability for concrete mixture, therefore, to solve this problem superplasticizers(chemical admixtures) without influencing other characteristics of concrete may introduce (Kamran , 2012; Vairagade et al., 2012).

2.1.5 Mechanical Properties of steel fiber reinforced concrete (SFRC)

2.1.5.1 Tensile Strength of SFRC

Typically, SFs have high tensile strength from 1000 to 3000 MPa and Young's modulus of 20000 MPa, specific gravity of 7.84, and elongation to failure 3-4 % (James and Beaudoin, 1990). The SFs have been employed in conventional concrete mixes, shotcrete and slurry-infiltrated fiber concrete.

Usually, content of steel fiber ranges from 0.25 to 2.0% by volume of concrete. SFs content in excess of 2.0% by volume generally cause to poor workability, but can be used successfully where the size of coarse aggregate is not larger than about 10 mm and paste content of the mix is increased. Moreover, content of steel fiber in concrete up to 1.5% by volume must be pumped by using pipes of 125 to 150 mm diameter (Campbell, 2010).

Actually, with the use of high volume fraction SFs in concrete, a notable increase in the tensile/flexural strength over and above the plain matrix was observed. Once the tensile capacity of the composite was induced, and adhesion and transformation of micro-cracks to macro-cracks happened. Fibers, depending on their length and bonding properties continued to resist crack opening and crack growth by effectively flaking across macro-cracks. This post peak macro-crack flaking was the primary reinforcement mechanisms in the majority of commercial fiber reinforced concrete composites (Banthia, 2012).

2.1.5.2 Flexural strength of SFRC

Ramakrishnan et al. (1980) observed that hooked SFs were better than the straight fibers in terms of producing a higher ultimate flexural toughness and flexural strength. As seen in Figure 2.5a, the utilize of hooked SFs in an amount greater than or equal to 80 Ib per cubic yard (about 0.6% by volume) resulted in a post-cracking strength nearly equivalent to or greater than the first-crack strength. The superiority of hooked SFs relative to straight SFs was also assured by Soroushian and Bayasi (1991), as seen in Figure 2.5b.

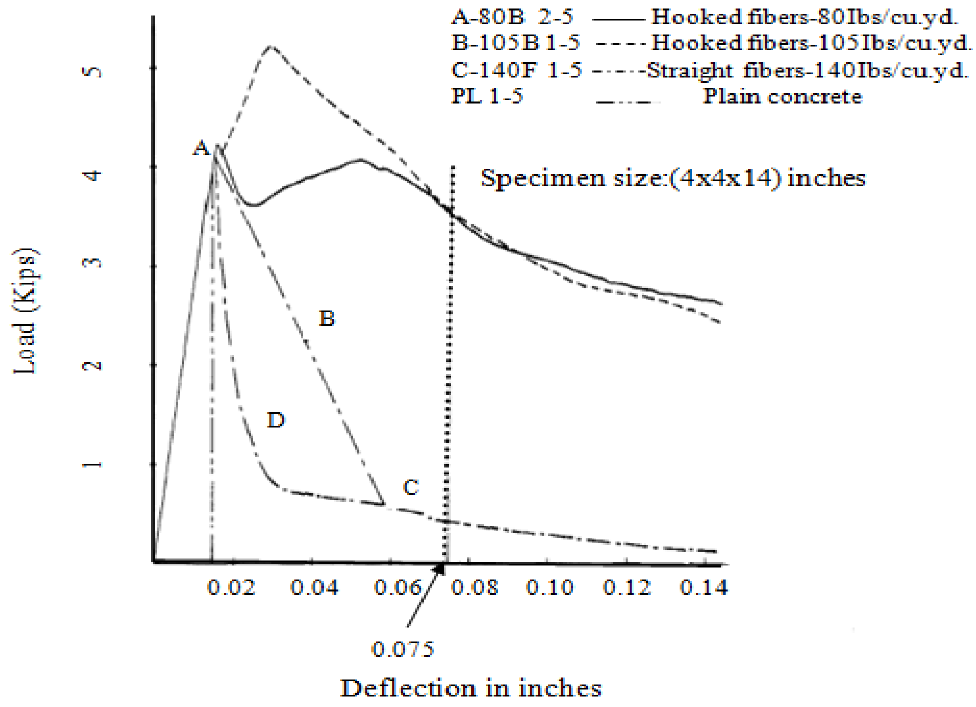

a)

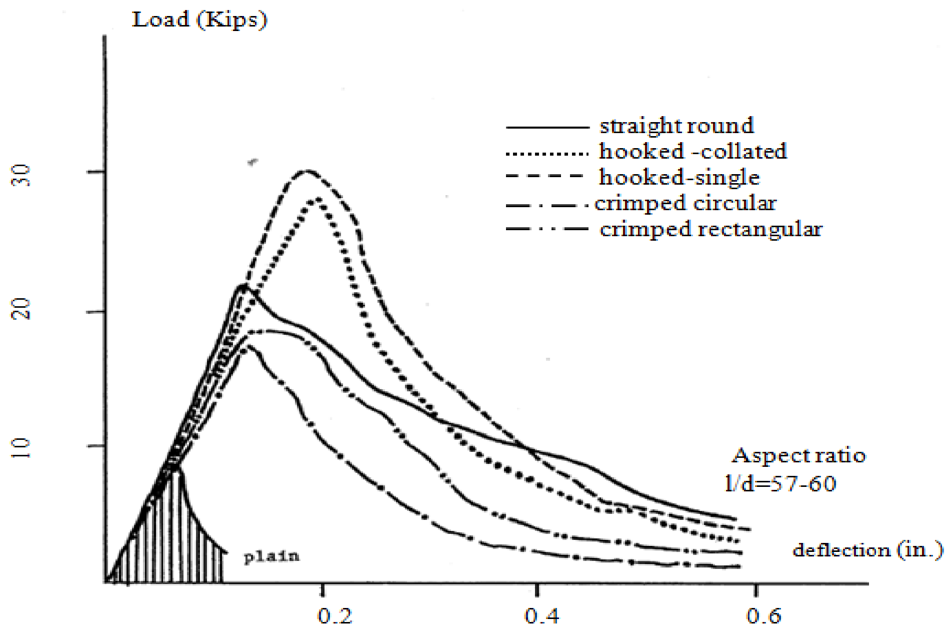

b)

Figure 2.5 Effect of hooked and straight steel fibers on flexural performance of concrete: a) from Ramakrishnan et al. (1980) and b) from Soroushian and Bayasi (1991)

Ganesan et al. (2006) analyzed the effect of SFs on the flexural behavior of concrete beams. Twenty beams were cast eighteen of beams with fibers and two without fibers was considered as a reference beams. The variables in their work were aspect ratio and percentage of volume fraction of fibers. The results showed the overall development in strain characteristics.

Veera (2012) conducted an experimental program to study the flexural behavior of simply supported beams by addition SFs and rice husk ash to high strength concrete. The experimental work carried out on twelve rectangular RC beams examined under two-point loading with different volume of SFs and longitudinal reinforcement. Moments and curvatures were computed from the experimental result and the moment-curvature diagrams were presented in their study. It was observed that with the use of SF, the beams behaved in a ductile manner even if the beams were over reinforced.

When adding SFs in concrete characteristics of concrete improved including flexural strength can be increased of up to 3 times more compared to traditional concrete, almost the fatigue resistance can be increased of 1.5 times in fatigue strength, greater resistance to collapse in case of a heavy impact, the composition become less porous, greater resistance against abrasion and spalling and shrinkage cracks can be decreased (Sreeja, 2013).

2.1.5.3 Shear strength of SFRC

Thomas and Ramaswamy (2007) studied about the shear strength with a presence or absence of SFs in eleven T-prestressed concrete beams which each beam has length 3850 mm and shear span –to – depth ratio was 2.65 to 1.59, respectively and then proved by using Response-2000 program, while the SFs were irregular distributed over a flange zone, web zone and entire section of beams, respectively. The authors observed the SFs which distributed over the web zone only of the beams having shear strength equivalent to the shear strength of beams included steel fibers at over full depth.

Greenough and Nehdi, (2008) carried out a detailed examination on the shear behavior of fiber reinforced self - consolidating concrete slender beams. The author noticed that the short discrete steel fibers could significantly develop the shear behavior and beams including 1% fiber content could obtain a 128% increase in shear capacity over that of the original beam without fibers.

2.1.5.4 Absorbed energy from SF addition

Naaman and Gopalaratnam, (1983) investigated the effect of strain rate of loading including impact on the bending properties of steel fiber reinforced concrete (SFRC) using an instrumented drop-weight impact machine. The increase in energy absorbed and composite flexural strength with loading rates was referred primarily to the strain rate sensitivity of both the matrix and the pull out resistance of the fibers.

Sreeja (2013) presented the experimental and analytical investigations of behavior RC beams reinforced by SFs subjected to cyclic of impact loading to study the effect of steel fibers distribution on the ultimate strength. The analytical investigations were carried out by 3D finite element ANSYS model. Experimental tests conducted on five beams in various proportions of SFs to establish load-deflection curves. The experimental and analytical results indicated that the composition behaved more ductility to resist repeatedly applied impact loading, greater resistance to cracking and crack propagation, increased extensibility and tensile strength, the fibers were able to hold the matrix even after progressive cracking, pronounced post – cracking ductility which was unheard of in conventional RC beam. Finally, increasing the SFs proportion in RC beam and decreasing in the spacing of stirrups revealed to increase the strength.

2.1.5.5 Compressive strength of SFRC

Despite by addition SFs throughout the members which contained conventional reinforcement bars, and whatever the content of SFs had a slightly impact on the static compressive strength, with improved in strength not be exceeded 25% (Johnston, 1974). It was confirmed by ACI 544, (1996) that the volume fraction 1.5% of SFs caused to increase the compressive strength from nil to 15 %. Figure 2.6 shows the stress-strain relationship of plain concrete 0.0-3.0% SFRC.

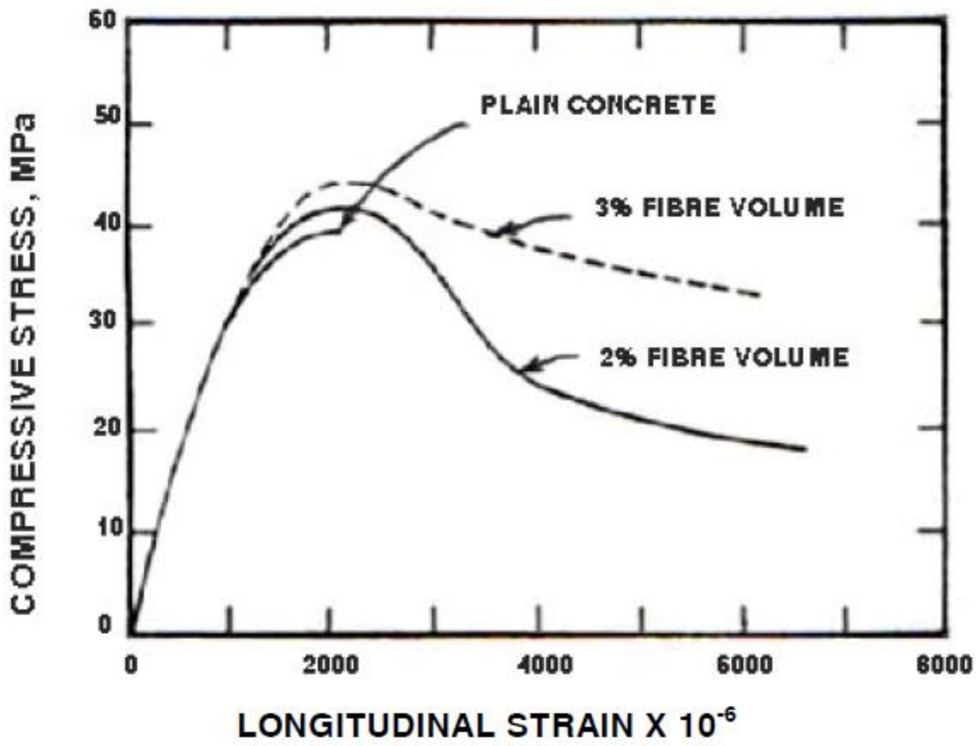

Figure 2.6 Stress-strain curves in compression for SFRC (Johnston, 1974)

2.2 Steel plate applications

The concern of strengthening of RC structures has increased in the last few years due to poor performance under increasing service loading in the form of excessive cracking and deflections, inaccuracy in design, excessive deterioration and the changing in use of construction. Therefore, externally bonded steel plates are one of methods for strengthening conventional R.C beams. The technique of epoxy-bonding steel plate to the tensile zone of RC beams has been examined as a technique to strengthen existing RC structures because it is easily to install and very successfully to increase the RC beams performance in ultimate flexural load. However, a problem that has been happened during the testing of RC with epoxy-bonded steel plate is separation of the plate from the beam at the ending of concrete compression failure (Hesham, 2010).

2.2.1 Method of connection of steel plate in tension face of RC structures

The late 1960s, several investigators dealt with the strengthening method that steel plates were adhesively bonded with epoxy resin adhesive at the lower part of RC beams. In those days, due to the fatigue deterioration of concrete decks and propagation of cracks were frequently found on the Japanese highway bridges, experimental researches on the external steel plate bonding method applying to the bridge decks were carried out in different studies (Ohta,1971; Ishitani,1975; Iioka et al. 1976; Iioka et al. 1977).

It is worth mentioning, the strengthening by external steel plate to the tension zone of RC beam are usually connected together by resin adhesive or steel anchor and resin adhesive together. If they are not, each element will act separately and thus the load carrying capacity of the beam is not greater than the sum of the individual capacities of the elements. In another way, if provision is made for the horizontal shear force, transformed between these two components, the total load capacity will be increased noticeably. Moreover, thickness of steel plate (ts) must not be exceeded 4 mm if the connection is only generated by glue, whereas, (ts) must not be exceeded 12 mm if the connection generated by glue and steel anchor together. Besides that, thickness of glue (tg) must be achieved between 1 and 3 mm because higher glue thick leads to a lower bond capacity between the external steel plate and RC beam, as shown in Figure 2.7, and taking into consideration, the surface of concrete must be roughness enough to achieve a best bonding with strengthened steel plate. Also, the strengthened steel plate must be coated to protect it from correction (Appleton and Gomes, 1997).

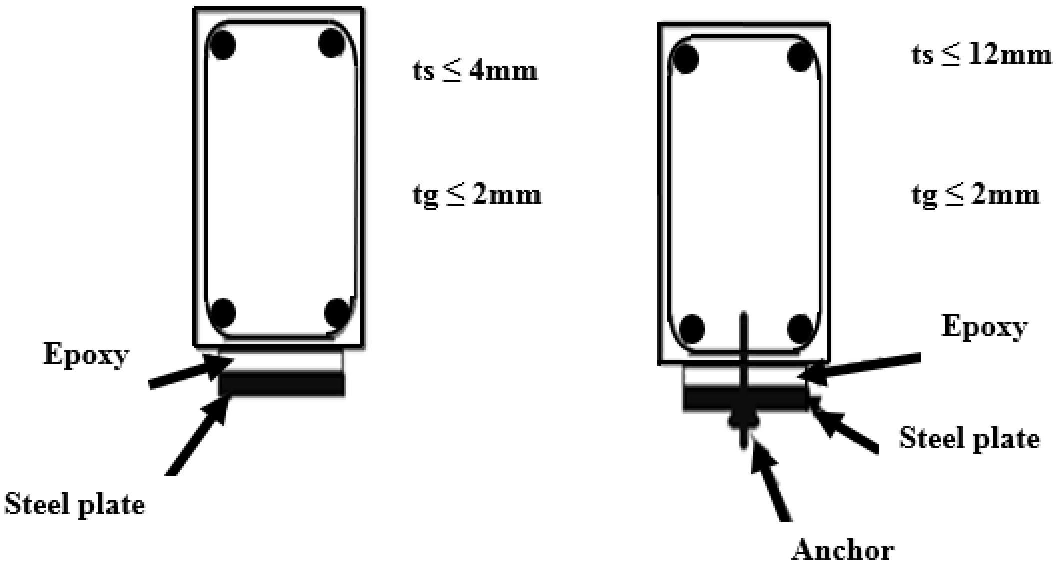

Figure 2.7 Flexural strengthening –recommended dimensions limits (Appleton and Gomes, 1997)

The more relevant resin adhesive properties for this type of application, which are given in the study of Appleton and Gomes (1997):

- Viscosity
- The hardening time
- Shear modulus of adhesive
- Modulus of elasticity
- Compressive strength
- Tensile strength

It is worth noting that the glue must not be used with ambient air temperature lower than 10°C (Appleton and Sliva, 1995). Some typical characteristics of resin adhesive, as shown in Table 2.3 (Goosey et al. 1999).

Table 2.3 Shows physical properties for resin adhesive (Goosey et al. 1999)

Characteristics of resin adhesive	Values
Tensile strength (MPa)	(350-600)
Modulus of elasticity (MPa)	500-20000
Maximum temperature during loading (˚C)	40-80
Temperature expansion coefficient (1/˚C.10-6)	25-30

Jones et al. (1988) measured the stresses generated due to bonding steel plate of simply supported reinforced concrete beams with epoxy-bonded plates on the tensile zone. Seven RC beams under three-point of loading were tested. Distributed strain gages at the end of steel plates and the centerline of the beam. Three beams were strengthened with the varying plate locations. Two utilized straight steel plates by addition of epoxy-anchor bolts at the plate curtailment.

The last two beams had a steel plate attached to the bottom and then had various size L-shaped anchor steel plates epoxy attached to the bottom plate which spreaded up the side of the beam. The first three beams failed by rupturing at the plate at the end. The two beams with epoxy anchors witnessed partial separation of the plates, with the beams finally failing by crushing of the concrete in the constant moment region. The L-shaped anchor steel plates were the most efficient strengthening system, with each beam strengthened in this way reaching full flexural capacity.

All the anchorage systems had similar stiffness, about 60% greater than a beam without steel plate. The three beams with only anchor steel plates had a sudden failure, but the addition of the anchor bolts resulted in a ductile failure for the two beams reinforced this manner (Jones et al. 1988).

Martins and Guimaräes (1996) conducted an experimental work on full- scale RC beams. Six beams with an effective span of 4800 mm and a 1200 mm long cantilever with a rectangular cross-section of 150x600 mm were examined. Four of the examined beams were strengthened using steel plates with a thickness of 3.34 mm without any external factors used for installation, while, the other two beams were pressed by external cage of rebars with overall cross-section dimensions of 200x700mm to anchorage the steel plate against the concrete surface to prevent air bubbles may be generated during the glue hardening period. Their emphasized on the need for appropriate anchorage devices must be used to ensure the steel plate connect perfectly on concrete surface to make the beam behave as a layered beam, thereby possible and acceptable as a warranty for ductility of the beam. Furthermore, in spite of the anchorage way was used in this work proven effective of anchorage the steel plate on concrete surface and made as one unit against the increasing of load but more difficult to apply in practice.

Calder (1979-1989) recorded the results of exposure experiments on un-reinforced concrete beams with overall dimensions 102x 102x508 mm, reinforced by externally mild steel plates with dimensions 38x3x508 mm, which were loaded in the mid-span of theses beams. These experiments were subsequently extended to contain another series of beams of dimensions 150x250x3500 mm which were reinforced by externally mild steel plates of dimensions 85x3x2800 mm.

Two different adhesive resins (kinds I and II) were utilized to attach the plates to the beams in the second series: half the number of these beams were loaded in such a way as to create cracking in the concrete before plating, and the other half of the test samples were loaded centrally after plating. The beams were retained under external load for up to 8 years. Light corrosion was noticed at the plate-resin interface of the beams attached with resin kind I, and the system performance of these beams was not believed to have been adversely affected by the 8 year exposure period. Premature failure of the beams with plates attached using resin kind II result to the conclusion that this kind of resin was of an unsuitable nature for such applications.

2.2.2 Cracks and deflection

The modes of failure and cracks are occurred by strengthened steel plate in tension zone of beam can be categorized into two groups (Teng et al.2003; Smith and Teng, 2003):

1) Shear cracks propagated along the connection zone between beam and plate due to the high interface stresses occurred at the near ends of the bonded plate, gradually may be induced separation concrete cover Figure 2.8a or separation between plate and concrete, as shown in Figure 2.8b.

2) Intermediate flexural or flexural-shear crack occurred due to interfacial debonding initiating in the high moment region and propagate towards one of the plate ends as shown in Figures 2.8c and 2.8d. When the distance between end of plate and the adjacent beam support is very small governed critical diagonal crack (CDC) debonding failure, as shown in Figure 2.8e, while increase the distance between them, the CDC may fall outside the plate region which causes to concrete cover separation, as shown in Figure 2.8a.

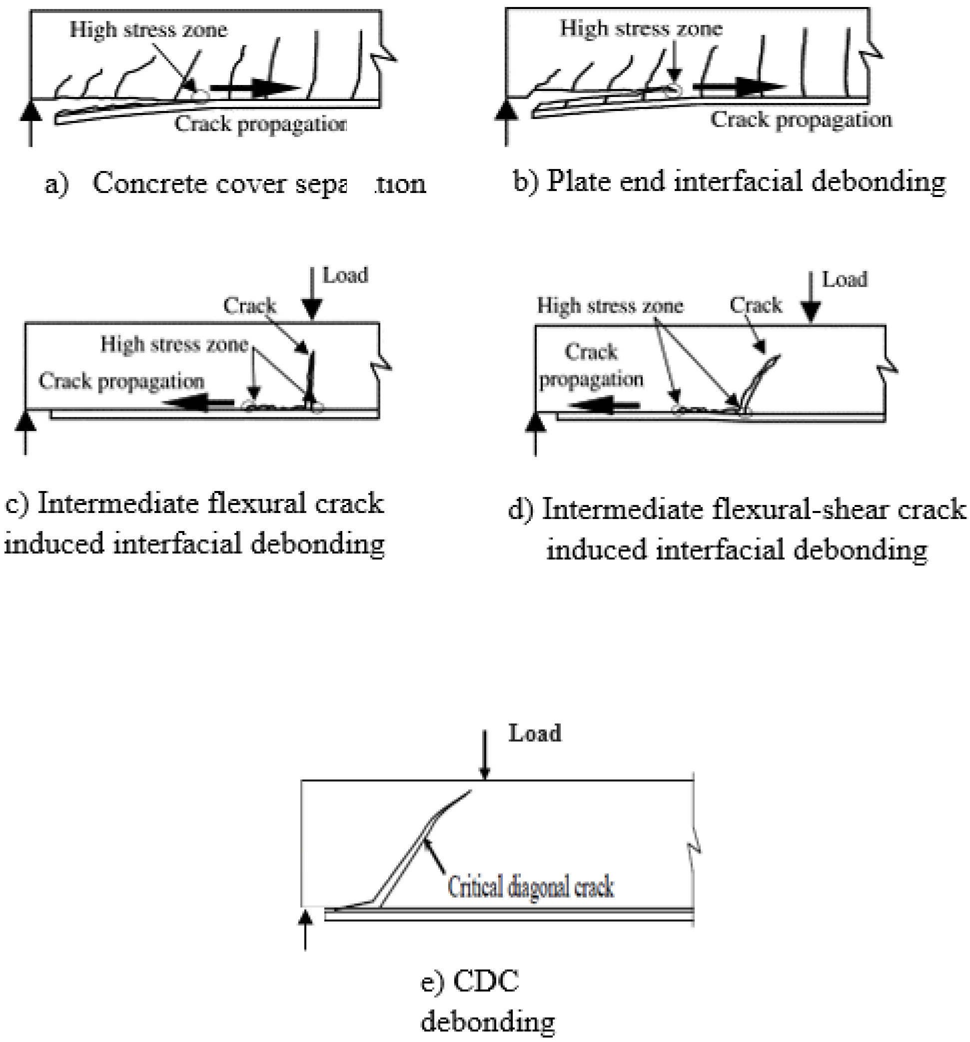

Figure 2.8 Failure modes of RC beams flexural-strengthened with steel plate (Teng, 2003; Smith and Teng, 2003)

Lioyd et al. (1982) noticed a uniformly distributed corrosion over the steel plate and appearance infinitesimal cracks in layer of glue when bonded externally with concrete were induced by migration of moisture from concrete mixture and penetrated through the glue. The authors were found the corrosion caused to decrease the bond strength between concrete and steel plate, in spite of appearance these cracks the bond strength was still much great than the shear strength of concrete.

Swamy et al. (1987) studied the effect of glued steel plates to tension face of RC beams on appearance of first cracking, crack propagation, deformations, and ultimate strength. Twenty beams were examined with 2500 mm length. The beams were examined as simply supported and loaded at third points. The thickness layer of glue and thickness of plate were variable each of them (1.5, 3, and 6 mm), but width of plate was constant. Only two beams were not plated and were utilized as control beams but one of them was covered with glue with a thickness of 3 mm in the absence of external plate. It was founded that the addition of glued steel plate to RC beam can reduce cracking propagation; deformations at all load steps and virtually increase their flexural stiffness. Modest delay of appearance first crack, and when the glue alone was exist. Crack propagation was observed to increase with increasing the plate and the glue thicknesses.

Swamy et al. (1995) studied structural behavior of externally bonded steel plated to the tension face of RC beams exposed in an industrial area directly and continuously without any maintenance for periods of 11 to 12 years. Eight beams were kept under sustained loading rigs and they were simply supported, and loaded at the third points for the whole exposure period and the other 13 were left unloaded were also simply supported. The bonded of steel plate to the tension face were consisted of three main plating strategies. The first strategy contained ten beams which were each strengthened with a single continuous plate. The second strategy contained six beams which had a attached single plate regime with lap plates at one or more locations. The third strategy contained of five beams which had two laminates of plates throughout their length. Tow plated beams were considered as a reference beams, one of them was tested with exposure to same circumference of pollution, while the other was tested under ordinary circumference. Crack widths and deflections at service load levels of beams examined after exposure were equivalent or less than those of the reference plated beam. Beams with a single continuous plate proved no inversely affect due to long-term exposure, and these beams carried a higher load about 10% more than that the others plated beam system.

Hussain et al. (1995) discussed preloading RC beams repairing by steel plates of differing thickness to the tension face. Strain gages were installed at the main reinforcement, upper surface of concrete in mid span and along the steel plate to determine strain distribution. All RC beams were preloaded to 85% of their ultimate load capacity, which the centerline deflection of 10 mm with loading applied at third points. The repaired RC beams were then reloaded to failure. They were observed deflection rate during loading, unloading, and reloading was 1 mm per min.

Seppo (1996) conducted an experimental work to determine the relationship between the width and thickness of the bonded steel plate on the tension face of RC and steel beams by using glue, and subjected to static and repeated loading. The two kinds of glue were utilized for bonding steel plate; Epoxy BI-R and Concressive 1380 for RC beams, while Araldite AV 129 HV 997 for steel beams with thickness of the glue layer after hardening was approximately 1 mm. The width of the steel plate was constant 100mm, while the thickness was varied from 2 to 10 mm. Their observed the ratio between the width and thickness of the attached steel plate must not be exceeded than 20.Furthermore, the existence of glue between the steel plate and concrete can be decreased the crack width and deflection in RC beams.

Hesham (2010) presented an experimental program to study the effect of increasing the compressive strength of the section and increasing the ratio of steel reinforcement on behavior of RC beams outwardly strengthened by glued steel plate at the lower tension zone of these beams. Ten beams with dimensions of 250 mm in height, 150 mm in width, and 2500mm in length, five of them were without external steel plate as considered reference beams, whereas the other five ones were supplied with steel plate with dimensions of 1mm in thickness, 100mm in width, and 2500 mm in length under two point loading till to failure were tested. Three values of compressive strength were utilized in his study which were (22, 45 and 71 MPa) as well as three ratios of steel reinforcement bars which were (0.01411, 0.02116 and 0.03445).

The experimental results revealed that the cracking load and the ultimate load can be improved up to (150% and 137%) respectively. As well, by increasing the section compressive strength all the properties of the strengthened beam can be increased whereas by increasing the reinforcement ratio with existence steel plate and increased of diameter and number of internal steel bars the deflection and cracking can be decreased to develop the elastic behavior of the beam.

Awadh et al. (2011) conducted an experimental work the possibility of reducing internal tension bars for RC beam and replacing by externally steel plate which it connected at the bottom face of beam. Six RC beams with dimensions 100x150x1500 mm under two point loading up to failure were tested. The researchers were depended on changing the dimensions of steel plate with increasing the plate width against its thickness and vice versa, where the width of plate ranged from 25, 50 and 75 mm, while thickness of plate ranged from 0.5,1 and 1.5 mm. The connection between externally steel plate and concrete surface of these beams was carried out by using adhesive resin, commercially named Top Bond 603. The data results asserted the possibility to decrease the amount of conventional tension reinforcement bars of RC beam with rate of up to 67% for steel plate was 0.5 mm in thickness and 75 mm in width compared with other plates beside that, significantly increased flexural strength contributed in decreasing in crack propagation along the beam.

2.2.3 Shear strength

Ziraba et al. (1994) introduced the guidelines for the design of RC beams with external steel plates bonded with epoxy. Three steps were determined as the major design procedure. The first step of design was assumed the failure occurrence under the steel plate yielding and the concrete crushing by using basic principles of reinforced concrete beam design. The second step must be checked the stresses generated at the interface between them and then compute the maximum distance between end of plate and the beam support depended on an allowable value coefficient of cohesion of concrete, glue and steel at the interface. Finally, the shear capacity of the beam was determined by using too the principles of RC beam design. Fifty RC beams 100 x 150 x 2250 mm were designed using this procedure and were tested up to failure load using four point loading. They found a good matching has achieved between experimental results and predicated procedure of design.

Aprile et al. (2001) compared between behavior of RC beams reinforced by elasto-plastic steel plates and elastic-brittle carbon laminates. They observed the bond stresses distributions is different for steel plates than for carbon laminate in shear span due the steel plates were approached to yield condition before the steel reinforcing bars inside the RC beam, on the contrary of strengthening by carbon laminates.

Arslan et al. (2008) introduced a 3D nonlinear finite element method to evaluate behavior of RC beams were strengthened by externally steel plate whether it was continuous along the lower surface of these beams or not. They concluded that the strengthened RC beams by this technique of bonding significantly improved the ultimate load –carrying of capacities of failure relative to original condition of RC beams and suggested a formulation for ultimate shear capacity of retrofitted beams except for beams which have steel plate expanded between support conditions.

Seema et al. (2013) conducted an experimental work to discuss the shear strength behavior resulted from reinforcing RC beams by externally steel plate at the web zones only. Twenty six of RC beams without and with internal shear reinforcement, different thickness of steel plates and different depth of steel plate respect to depth of web of retrofitted RC beams beside that they were adopted the principle of connection the steel plates on epoxy adhesive. The researchers observed the shear strength of a beam with bonded steel plates is increased with increasing plate depth and thickness across the beam section, besides that, the effect of depth of steel plates has more impact on shear strength rather than the thickness of plates.

2.2.4 Flexural strength

Raoof and Zhang (1997) employed non-linear finite element method on RC beams with externally bonded steel plates to study the relationship between the ratio of internal reinforcement to ratio of steel plate area and effect on the flexural stiffness of these beams. They found that inclusion of external steel plates causes to increase in the generally flexural stiffness of the beams, but increased in the flexural stiffness was more marked for under-reinforced beams. Moreover, based on numerical results, in spite of, they assumed full bond between concrete and external steel plate up to the ultimate load and plane sections remain plane after bending the cross-section of beam experiencing significant distortion due to curvature.

Suguna et al. (2006) presented the results of analytical and experimental studies conducted on RC beams with externally bonded corrosion resistance stainless steel plate reinforcement. The experimental studies carried out on twelve RC beams to determine improvements in their flexural capacity, deformation and ductility properties. The analytical model implemented in C^{++} programming language for computing the load deflection behavior. They found a very good agreement has been accomplished between the results computed by the model and experimental results.

CHAPTER 3

METHODOLOGY

3.1 General

Rehabilitation and repair of structures are fundamental not only to utilize them for their intended service lifetime but also to guarantee the safety and serviceability of the associated ingredients so that they meet the same requirements of the structures built today and in future. The current study has highlighted two strategies to improve the function, performance, strength, and stiffness of RC beams. The first one is the use of steel fibers throughout the beams while the second one is the utilization of the external steel plate in tension zone. Due to the progressing in software and computational features, a general-purpose nonlinear finite element analysis program of ANSYS (SAS, 2005) has been employed. In the following sections, more detailed explanations on the methodology of the study are given.

3.2 Specimens details

In this investigation, a full-size RC beam was used, while its dimensions of the beam were 200 x 800 mm cross section and 6500 mm long. The beam was reinforced with 3Ø 16 mm and 2Ø 10 mm as main reinforcements and stirrups were with Ø6 mm at 250 mm. The compressive strength and the modulus of elasticity of concrete were 3337, and 2715 Ton/m^2, respectively. The boundary conditions of the beam were assumed as a simply supported. The load was applied at the middle span of beam, as shown in Figure 3.1.

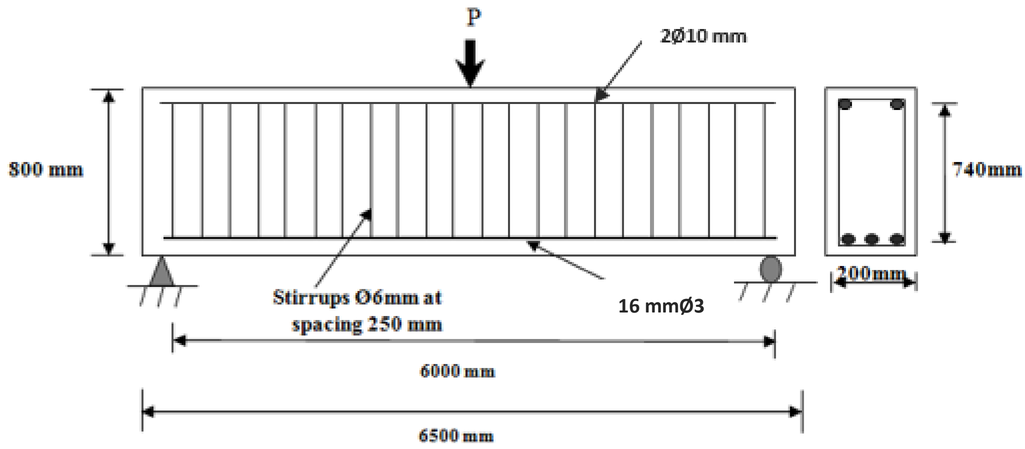

Figure 3.1 The dimensions and details of RC beam

The first procedure was used to improve the flexural behavior of strengthen the prescribed RC beam as shown above was by inserting the steel fibers of various volume ratios of 0.5, 1.0, and 2.0%, respectively throughout it. The steel fibers that used in this investigation were straight end and with aspect ratio of 80/50, as shown in Figure 3.2.

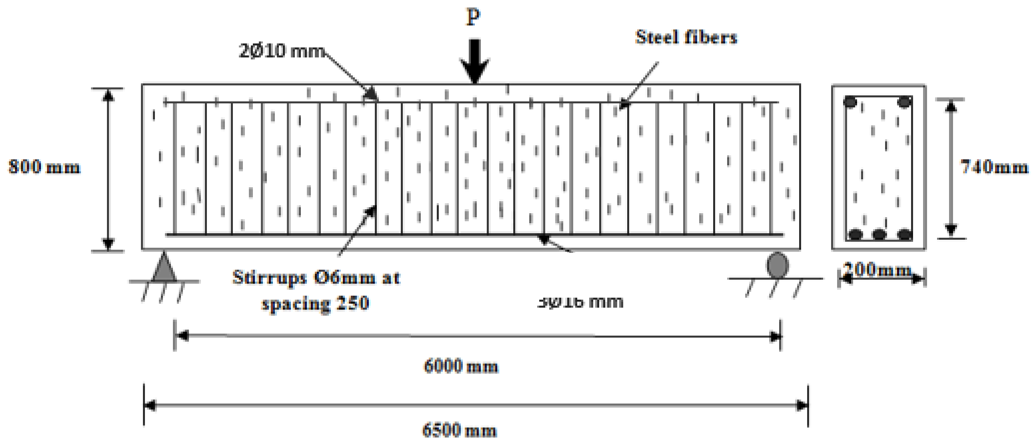

Figure 3.2 Strengthening of RC beam by steel fibers

While the second procedure was of strengthening the RC beam by covering steel plate at the lower face of the beam extended between two supports with different thicknesses of 1 mm, 2 mm, and 3 mm, respectively, but knowing that other dimensions and properties of steel plate were considered as constant at each stage of strengthening and bonding progress between RC beam and steel plate was by using glue with thickness of 1.0 mm, as depicted in Figure 3.3.

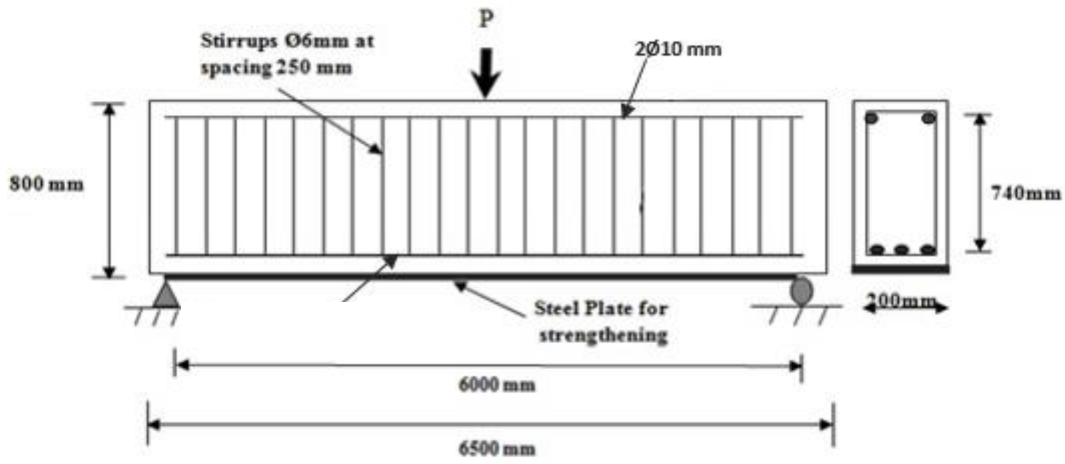

Figure 3.3 Strengthening of RC beam by externally steel plate

3.3 ANSYS Finite Element Model

The ANSYS program introduces a wide range of options concerning element types, material properties, auto-meshes, and graphics to speed the analyses. Therefore, the structural system modeling is based on utilizing of this commercial software. All program's inputs have been discussed in this chapter with details including element types, real constant, material properties, meshing, boundary condition, and applied load, beside that nonlinear analysis procedures and convergence criteria.

3.3.1 Element Types

3.3.1.1 Concrete

The current analysis used a principle of uniaxial stress-strain relationship (Saenz and Luis, 1964) for compression behavior of concrete all the details about the formation illustrated in Appendix. So that the concrete in ANSYS program was modeled as a solid element (SOLID65). Eight nodes were required for this element as shown in Figure 3.4. Each node had three degrees of freedom, translations in the nodal x, y, and z orientations. The element was capable to represent the plastic deformation, and cracking in three orthogonal orientations.

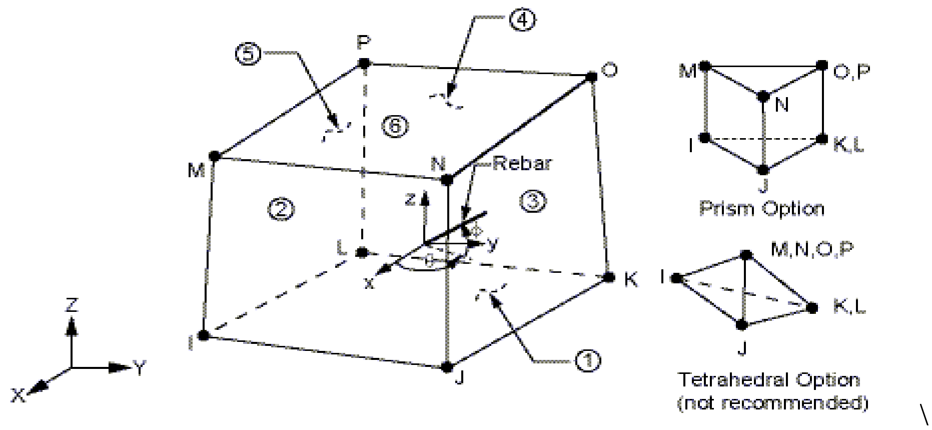

Figure 3.4 Solid65 element (SAS, 2005)

3.3.1.2 Steel reinforcement

A link element, link8 as illustrated in Figure. 3.5 was used to model the steel reinforcement (main reinforcements and stirrups reinforcement). The link element had two nodes with three degrees of freedom at each node, translations in the nodal x, y, and z orientations.

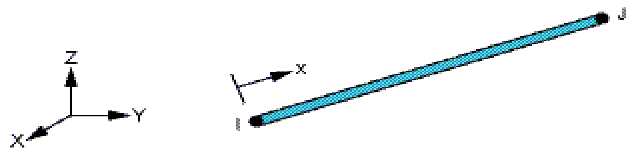

Figure 3.5 Link8 element (SAS, 2005)

3.3.1.3 Steel Plate for strengthening

SHELL181 as shown in Figure 3.6 was used to model the steel plate for strengthening on the RC beam. Four nodes were required for this element. Each node had six degrees of freedom, translations in the nodal x, y, and z orientations and rotations about the x, y, and z-axes. The element was suitable for modeling a sandwich structure and analyzing thin to moderately-thick shell structures.

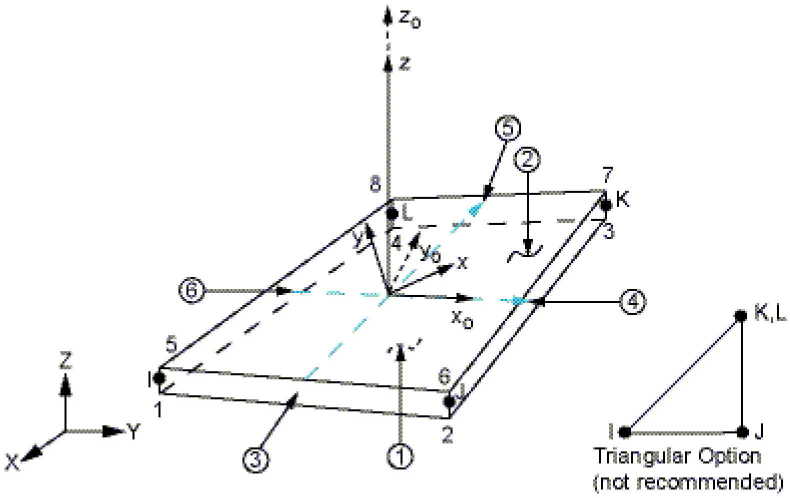

x_o = Element x-axis if ESYS is not provided.

x = Element x-axis if ESYS is provided.

Figure 3.6 Shell181 element (SAS, 2005)

3.3.1.4 Resin adhesive

A substructure, MATRIX50 that was treated as a single element. The Matrix50 element could substantially decrease the cost of many analyses. Multiple load vectors might also be inserted with the substructure matrices, thus allowing various loading conditions. The degrees of freedom were the master degrees of freedom limited during the generation pass. Figure 3.7 shows the Matrix50 element.

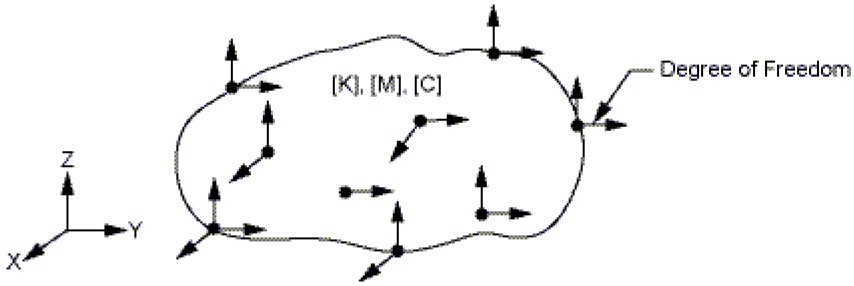

Figure 3.7 MATRIX50 element (SAS, 2005)

3.3.1.5 The support and loading plates

A solid element, SOLID45 is shown in Figure 3.8 was used to create the support and loading plates on beam. The SOLID45 element had eight nodes with three degree of freedom at each node which was translations in the nodal x, y, and z orientations. In current study, thick steel plates for SOLID45 with appropriate dimensions were used.

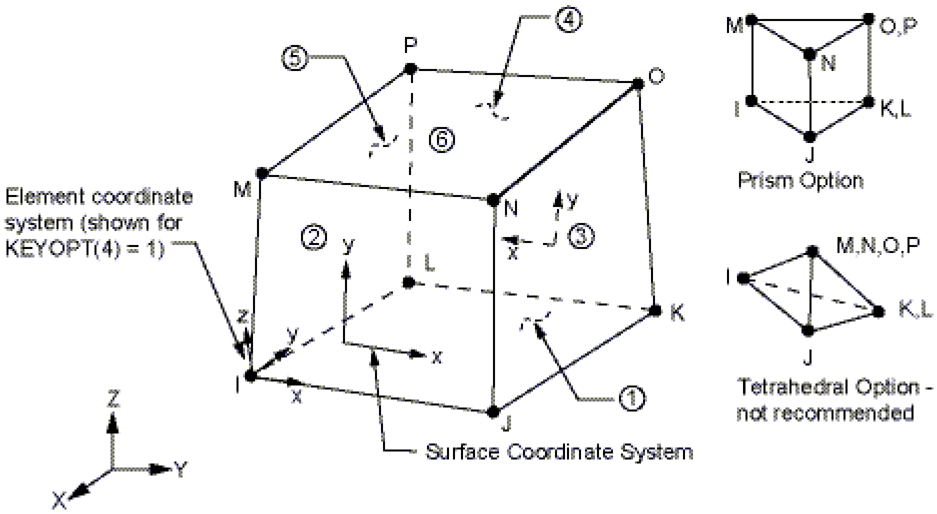

Figure 3.8 SOLID45 element (SAS, 2005)

3.3.1.6 CONTA174 and TARGE170

A CONTA174 was utilized to illustrate contact and sliding between 3D "target" surfaces determined by this element. Contact happened when the element surface permeated one of the target portion elements (TARG170) on a specified target surface. The CONTA174 element has eight nodes. The target surface (TARGE170) was discredited by a set of target portion elements and was paired with its related contact surface by sharing real constant set. The geometry, node positions, and the coordinate system for CONTA174 and TARGE170 elements are shown in Figure 3.9.

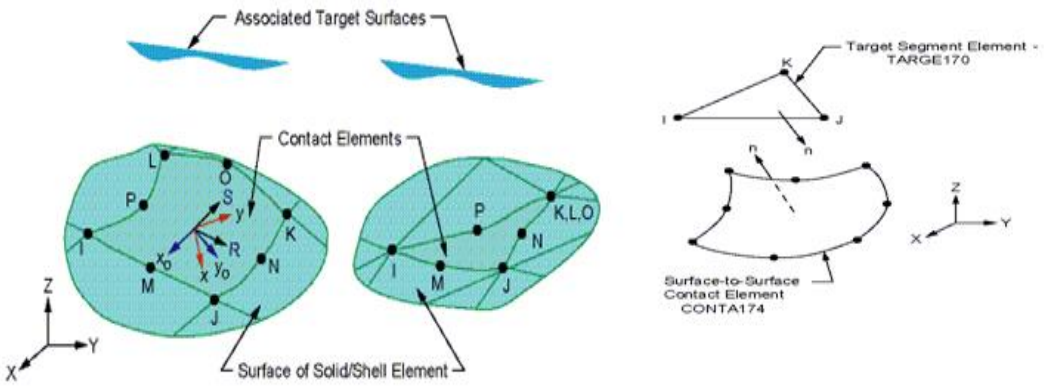

Figure 3.9 CONTA174 and TARGE170 elements (SAS, 2005)

3.3.2 Real Constants

The real constants for this analysis are shown in Table 3.1. Note that individual elements consist of different real constants. No real constant set exists for the Matrix50 element and Solid45.

Table 3.1 Real constant for the current models

<table>
<tr><td>Real constant set</td><td colspan="2">Element type</td><td colspan="3">Constant</td></tr>
<tr><td rowspan="5">1 (concrete)</td><td colspan="2"></td><td>Real constant for Rebar 1</td><td>Real constant for Rebar 2</td><td>Real constant for Rebar 3</td></tr>
<tr><td rowspan="4">Solid 65</td><td>Material number</td><td>3*</td><td>3*</td><td>3*</td></tr>
<tr><td>Volume Ratio</td><td>variable</td><td>variable</td><td>variable</td></tr>
<tr><td>Orientation Angle</td><td>0</td><td>90</td><td>0</td></tr>
<tr><td>Orientation Angle</td><td>0</td><td>0</td><td>90</td></tr>
<tr><td rowspan="2">2 (main reinforcement)</td><td colspan="2" rowspan="2">Link8</td><td colspan="2">Cross-sectional area (m^2)</td><td>7.603E-4</td></tr>
<tr><td colspan="2">Initial strain (m/m)</td><td>0</td></tr>
<tr><td rowspan="2">3 (stirrups reinforcement)</td><td colspan="2" rowspan="2">Link8</td><td colspan="2">Cross-sectional area (m^2)</td><td>5.027E-05</td></tr>
<tr><td colspan="2">Initial strain (m/m)</td><td>0</td></tr>
<tr><td rowspan="4">4 (Steel plate for strengthening the beam)</td><td colspan="2" rowspan="4">Shell181</td><td colspan="2">Shell thickness at node I(m)</td><td>variable</td></tr>
<tr><td colspan="2">Shell thickness at node J(m)</td><td>variable</td></tr>
<tr><td colspan="2">Shell thickness at node K(m)</td><td>variable</td></tr>
<tr><td colspan="2">Shell thickness at node L(m)</td><td>variable</td></tr>
</table>

From Table 3.1, the values of real constant set1 (Material number, volume ratio, and orientation angles) were specified for the strategy of strengthening RC beams by adding steel fibers only except this strategy of strengthening all these values were assumed to be zero.

On the other hand, the material number represents the type of material for reinforcement (3* which indicates the steel fibers material number). The volume ratio represents the ratio of volume steel fiber to the volume of concrete (when the volume of steel fibers was 0.5, 1.0, and 2.0%, respectively to the total volume of concrete, the volume ratio must be entered as 5.2E-03, 1.04E-02, and 2.08E-02, respectively.

It was assumed the orientation angles represented the orientation of the steel fibers as smeared layers in concrete element. ANSYS (SAS, 2005) lets the user to insert three rebar materials in the concrete. Each material corresponds to x, y, and z orientations in the element as shown in Table 3.1.

In addition, from Table 3.1 the real constant sets 2 and 3 were identified for the Link8 element. Values for cross-sectional area and initial strain were inserted. Cross-sectional areas in sets 2 and 3 refer to the main reinforcement and stirrups reinforcement, respectively. A value of zero was inserted for the initial strain due to the fact that there was no initial stress in the reinforcement. Finally, set 4 was defined for the shell181 element with regard to steel plate. Values of thickness of each node inserted. In this study, the thickness of steel plate was variable and could be defined from the user. The thickness of steel plate for strengthening was 0.001, 0.002 and 0.003 m, respectively. It was worth to mention that real constant set 1, 2, 3, respectively which used the strategy for strengthening RC beams by adding steel fibers in soffit of these beam, while the real constant set 1, 2, 3 and 4 respectively that used in strengthening RC beams by steel plate.

3.3.3 Material Properties

Parameters needed to determine the material models can be illustrated in Table 3.2 there are multiple parts of the material model for each element in model. Material Model Number 1 indicates the Solid65 element. The Solid65 element needs linear isotropic and multi-linear isotropic material properties to correctly model concrete. The multi-linear isotropic material employs the von Mises failure criterion along with the (Willam and Warnke, 1974) model to determine the failure of the concrete. In the present study, EX was defined as the modulus of elasticity and PRXY was defined as Poisson's ratio in Solid65. They were 2E6 Ton/ m^2 and 0.2 respectively, as illustrated in Table 3.2.

The equations of the uniaxial stress-strain relationship for the concrete model, as shown in Appendix. Typically, the shear transfer coefficients ranged from 0.0 to 1.0, with 0.0 was illustrated a smooth crack (complete loss of shear transfer) and 1.0 was illustrated a rough crack (no loss of shear transfer). The shear transfer coefficients for open and closed cracks were specified using the work of (Kachlakev, 2004). No deviation of the response happened with the change of the coefficient.

In this study, the coefficients for the open and closed cracks were set to 0.5 and 1.0, respectively, as listed in Table 3.2.

From Table 3.2, the material model number 2 refers to the Link8 and Shell181 element. In the beginning, these element were assumed as linear isotropic elements with EX=2E7 Ton/m² and PRXY=0.3 and bilinear isotropic properties to correctly model steel with yield stress (fy) and tangent modulus (E_t) were 36000 Ton/m² depend on von Mises failure criteria.

Material model number 3 refers to steel fibers, the behavior of steel fibers inside the concrete element were assumed similar to a large extent the behavior of the Link8 and Shell181 element except values in bilinear isotropic phase were fy=66000 Ton/m² and E_t=1050000 Ton/m², respectively, depend on properties of steel fibers .

Material Model Number 4 refers to Matrix50, the Matrix50 was modeled as a linear isotropic element with EX=250 Ton/m² and PRXY=0.41. The unixial tension strength and unixial compression strength was inserted as 2.8 and -1, respectively (Kachlakev et al. 2001). The material model number 5 indicated to solid45 which it was assumed as a linear istropic element only with EX=2E7 Ton/m² and PRXY=0.3 It was worth that notably, the material model number 1, part of material number 2 regard to Link8, 3 and 5 which used for strategy of strenghtening RC beams by steel fibers,while material model number 1, 2, 4 and 5 specified for for strategy of strenghtening RC beams by steel plate, as shown in Table 3.2.

Table 3.2 Material properties for the current models

Material Model Number	Element Type	Material Properties						
1	Solid65	Linear isotropic		Multi-linear Isotropic			Concrete	
		EX	3E6	No. of point	strain	stress	ShrCf-Op	0.5
		PRXY	0.2	Point1	0.001	2000	ShrCf-C1	1
				Point2	0.002	2500	UnTensSt	2.8
				Point3	0.0035	2500	UnCompSt	-1
							BiCompSt	0
							HydroPrs	0
							BiCompSt	0
							UnTensSt	0
							TenCrFac	0.6
2	Link8and shell181	Linear Isotropic		Bilinear Isotropic				
		EX	2E07	Yield Stss	36000			
		PRXY	0.3	Tang Mod	36000			
3	Steel fiber	Linear Isotropic		Bilinear Isotropic				
		EX	2E07	Yield Stss	66000			
		PRXY	0.3	Tang Mod	105000			
4	Matrix50	Linear Isotropic						
		EX	250					
		PRXY	0.4					
5	Solid45	Linear Isotropic		Bilinear Isotropic				
		EX	2E07	Yield Stss	36000			
		PRXY	0.3	Tang Mod	36000			

3.3. Meshing

To get ideal results from the concrete element, it should be used mapped command for meshing. Thus, the mesh was established to rectangular elements were formed as shown in Figure 3.10. No mesh of the reinforcement is required due to individual elements were generated in the modeling through the nodes generated by the mesh of the concrete volume. After that, the volume sweep command was utilized to mesh the steel plates which were used for loading and supports to match each elements and nodes with concrete elements and nodes, as illustrated in Figure 3.11. Besides that, the distribution of elements in steel plate that used to strengthen the beam based on the distribution element in concrete. Therefore, no need also meshing this component. The total number of elements in this investigation was 6058 element.

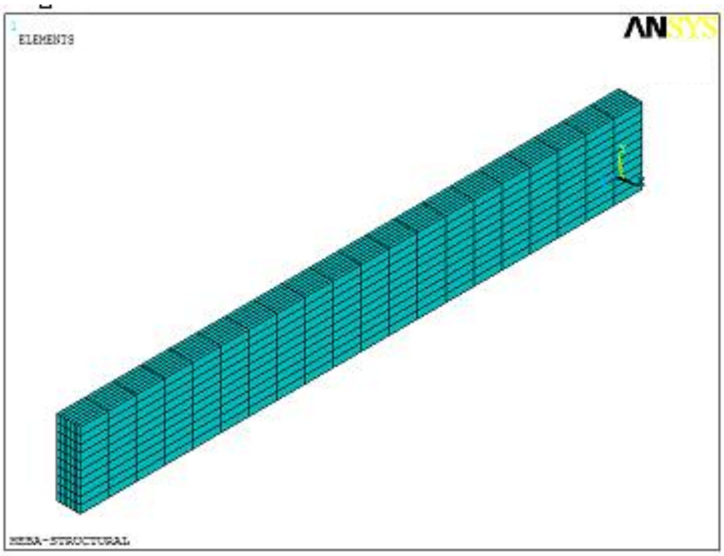

Figure 3.10 Mesh of concrete before using the steel fiber or steel plate

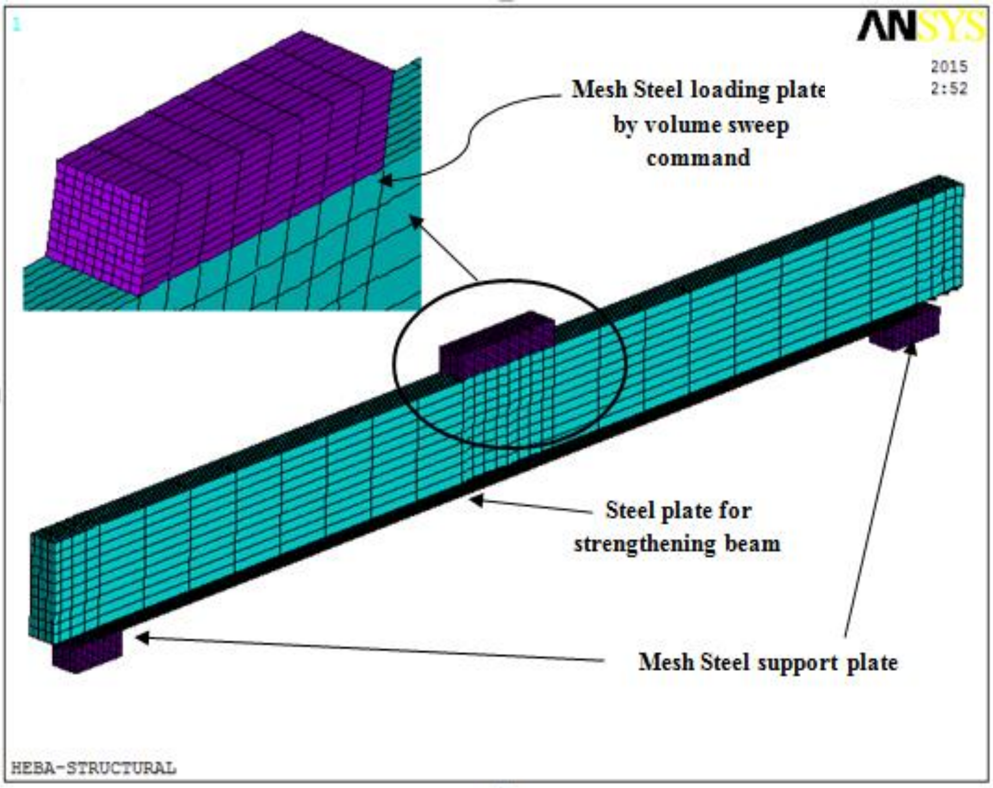

Figure 3.11 Illustration of the mesh in concrete with steel plates at loading zone and support conditions

3.3.5 Boundary Conditions and Loads

To obtain proper results the constrains of boundary conditions should be defined accordingly. A simply supported beam system was modeled in this investigation, as shown in Figure 3.12, and as well known, a hinge support condition constraints of X-direction and Y- direction, while a roller support condition constraints in Y- direction only, therefore these conditions were applied in current model at each node along the line connection between steel plate which it used to strengthen beam and steel plate of supports.

From Figure 3.12, the point-load (P) was applied on nodes across the entire centerline of the steel plate which it used for loading with less intensity at each edge to prevent unexpected hairline cracks at the top surface of concrete might be affected on the results of model.

In current study, it was supposed the final stage of loading with high load value at a 2000 Ton (fictitious value of final load) on all examined beams because the lack of expectation at any load might be failed these beams. However, all beams in this study were failed much earlier on supposed final stage for loading

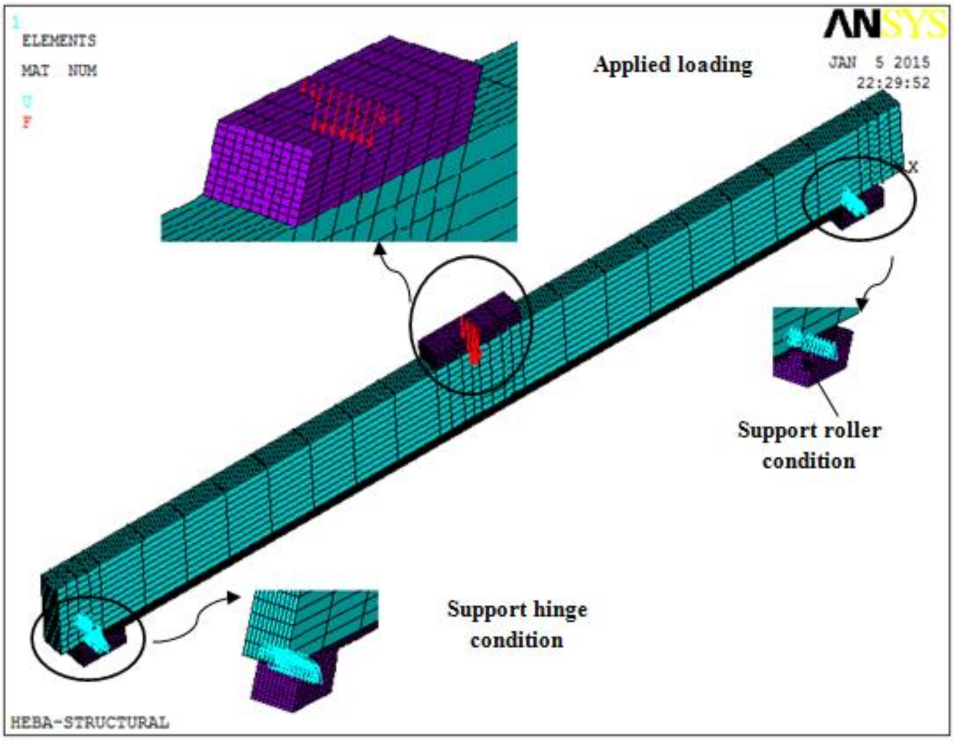

Figure 3.12 Boundary condition of the beam

3.3.6 Approach of solution

In the present study, the Newton–Raphson method was utilized to solve the nonlinear properties problem that the total load was divided into a sequence of load increments defined as load step, the load step was used 5 Ton in current model. At the accomplishment of each incremental solution, the stiffness matrix of current model was modified to indicate nonlinear changes in beam stiffness before continuance to the next load increment. The convergence of Newton-Raphson method was achieved at the end of each load step within tolerance limits (The default of tolerance was 0.001 for both displacement and load), as shown in Figure 3.13.

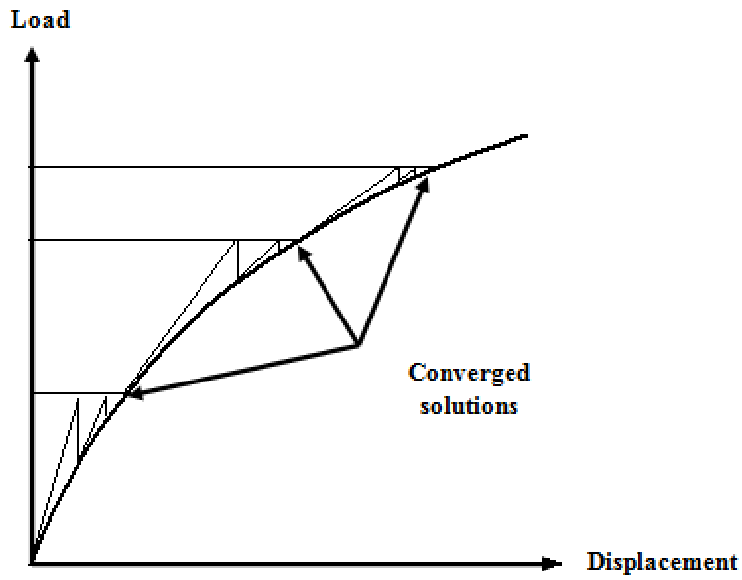

Figure 3.13 Newton–Raphson iterative solution (3 load increments) (SAS, 2005)

CHAPTER 4

RESULTS AND DISCUSSION

4.1 General

The current research consists of examining seven RC beams. The first beam is conventional RC beam without either addition of steel fibers or strengthening by bonding a steel plate. This beam was used as a reference beam (RB) while the other six beams were divided into two groups, the first group contains three beams (RB-SF0.5, RB-SF1.0, and RB-SF2.0) having different volume fractions of steel fibers (0.5, 1.0, and 2.0%), respectively, and the second group contains also three beams (RB-SP1, RB-SP2, and RB-SP3). They strengthened by bonding a steel plate at the lower tension face with steel plate thickness of 1, 2, and 3 mm, respectively. After that all beams were examined under a point load at the middle span of each beam until approaching the failure to study the characteristics of some parameters which were deflection, ductility, crack pattern, and mode of failure.

Validation of the current ANSYS models used for the RC beams by the addition of steel fibers or by bonding steel plate at the lower tension face were conducted with previous experimental studies of Ranjitsinh and Kulkarni (2014) and Awadh et al. (2011), respectively.

4.2 Strengthening RC beam with steel fiber

Many challenges faced the technique of adding steel fibers in RC beam when it applied in ANSYS model including aspect ratio of steel fibers and distribution of steel fibers through the beams make this technique more complicated. The results consist of deflection, ductility, besides that crack pattern and mode of failure for RC beam by addition of steel fibers with different proportions were displayed in this part.

4.2.1 Load -deflection relationship

From Figure 4.1 and Table 4.1, it was observed that the increasing the ratio of volume fraction for steel fibers in RC beam was accompanied by increasing of ultimate failure load. The results of ultimate failure load values at 18.9 tons, 20.4 tons, and 21.3 tons for beams RB-SF0.5, RB-SF1.0, and RB-SF2.0, respectively; while the ultimate failure load for beam RB at 17.5 tons only. This was due to the increase in tensile strength of concrete with the existence of the steel fibers through it, beside that the steel fibers worked as small bridges through retrofitted RC beams during the increasing of load and fill a part of the voids which generated into concrete matrixes so that, extra strength was added for traditional RC beam. Notable, the maximum percentage delay of appearance ultimate failure was 21.7% for the beam (RB-SF2.0) relative to beam (RB), as shown in Table 4.1.

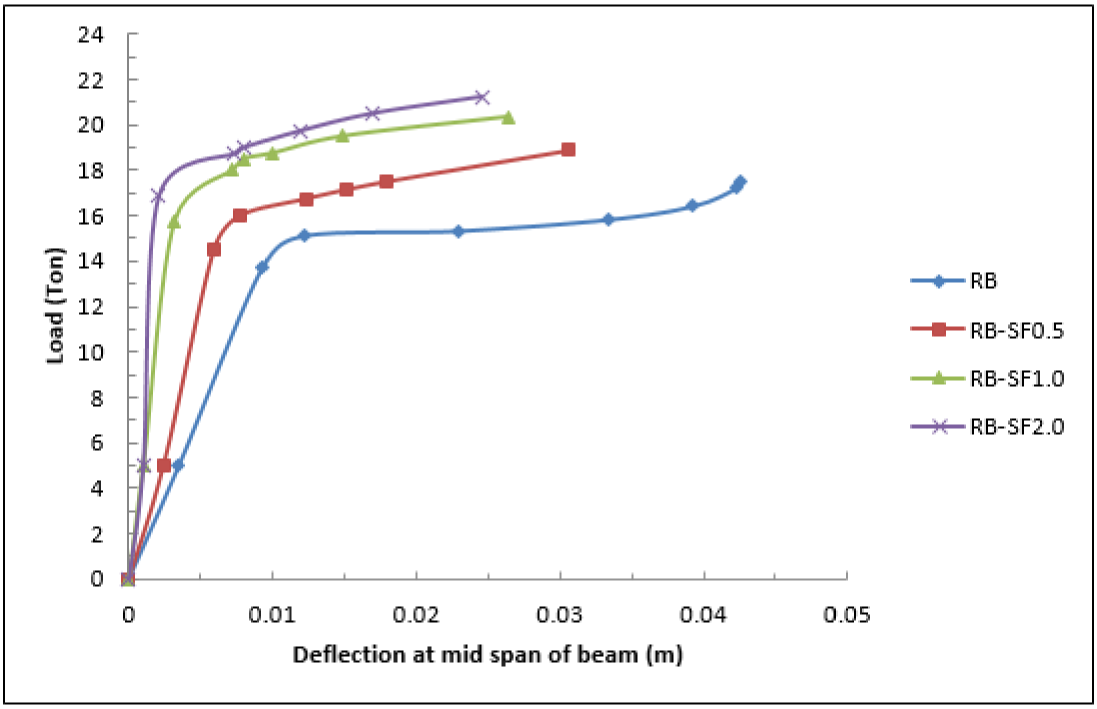

Figure 4.1 Relationship between load-deflection for RC beams with and without steel fiber

Besides that, from Table 4.1, it was illustrated that increasing the ratio of volume fraction for steel fibers to the beam (RB) had slightly effect on delay in appearance of first crack values. The appearance of first crack for beams (RB-SF0.5, RB-SF1.0, and RB-SF2.0) occurred at loads 4.5 tons, 4.8 tons, and 4.9 tons respectively whereas the appearances of first crack for beam (RB) occurred at load 4.4 tons.

This was due to the fact that the addition of steel fibers had no main effect on the pre-cracking strength of RC beam and even when used a high volume fraction of steel fibers. In current study, the first crack was occurred at the bottom face of all beams and the mid-span for all beams in this group. In addition, the percentage delay in appearance of first crack for the beams (RB-SF0.5, RB-SF1.0, and RB-SF2.0) were 2.3%, 9.0%, and 11.4%, respectively respect to the beam (RB).

Table 4.1 The results of the first crack and ultimate failure load for the first group of the beams

Beam	Appearance of First crack at Load (Ton)	Percentage delay of appearance first crack (%)	Failure Load (Ton)	Increment of ultimate failure load (%)
RB	4.4	——	17.5	——
RB-SF0.5	4.5	2.3	18.9	8.0
RB-SF1.0	4.8	9.0	20.4	16.6
RB-SF2.0	4.9	11.4	21.3	21.7

4.2.2 Ductility

Usually, the ductility is computed by dividing the value of deflection at failure per the value of deflection at yield state at the mid-span of beam and this known as deflection ductility.

In the present study, showed the results showed for all the upgraded beams by addition of steel fibers (RB-SF0.5, RB-SF1.0, and RB-SF2.0) became more ductility than that the beam (RB), as shown in Table 4.2. This was because of reducing the stress in the tension zone on internal reinforcement In other words, decreasing the yield strength in steel bars contributed in increasing the ductility (ACI, 2002) so that, the existence of steel fibers in RC beam allow a redistribution of stresses even when used at a low level of content.

Table 4.2 Deflection characteristics of RC beams

Beam	Deflection at yield Δ_y (m)	Deflection at Failure Δ_u (m)	Deflection ductility (Δ_u/ Δ_y)	Ratio of deflection ductility for beams
RB	0.0125	0.0426	3.4080	1
RB-SF0.5	0.0078	0.0361	4.6282	1.350
RB-SF1.0	0.0053	0.0264	4.9811	1.460
RB-SF2.0	0.0048	0.0246	5.1250	1.500

It was worth noting from Table 4.2 that the increasing of steel fiber content in the RC beam was followed by increasing the ratio of deflection ductility (Ratio of deflection ductility defined as deflection ductility of upgraded RC beam by adding steel fibers through it (RB-SF0.5, RB-SF1.0, and RB-SF2.0) per deflection ductility of the reference beam (RB)).

4.2.3 Vertical Deflection

Figures 4.2 to 4.5 depict the values of vertical deflection between two support conditions for the beams (RB-SF0.5, RB-SF1.0, and RB-SF2.0, respectively) at ultimate flexural load. From these figures, it was clear that the ratio of volume fraction of steel fibers had a significant impact on the vertical deflection values.

Progressively reducing of the vertical deflection values were accompanied by increasing the ratio of volume fraction for steel fibers because the existence of steel fibers through RC beam made the beam more stiffness. Besides that, the steel fibers were filled vastly of gaps that generated in concrete mixture thereby the strengthened RC beam by adding steel fibers through it became more resilient for successive increasing of load during the test compared with traditional RC beam.

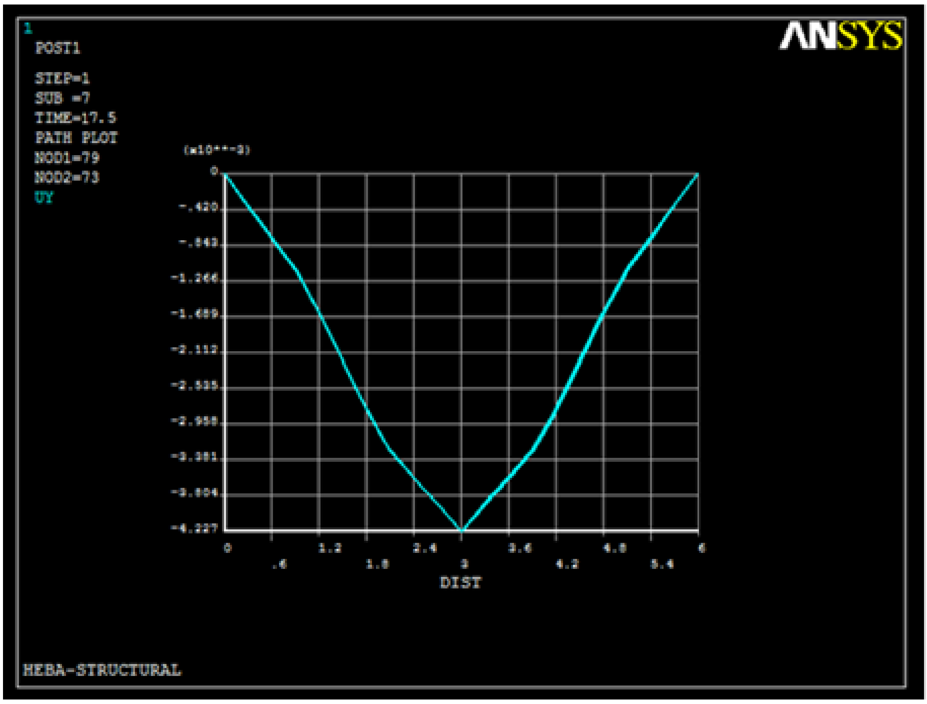

Figure 4.2 Showing the vertical deflection between two support conditions for the beam (RB) at failure load

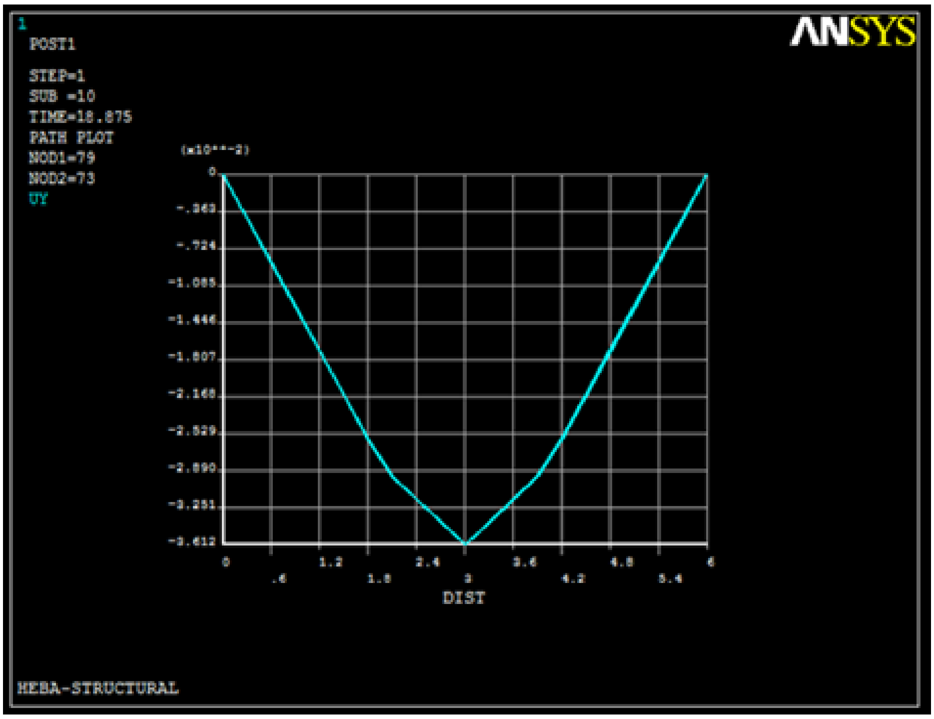

Figure 4.3 Showing the vertical deflection between two support conditions for the beam (RB-SF0.5) at failure load

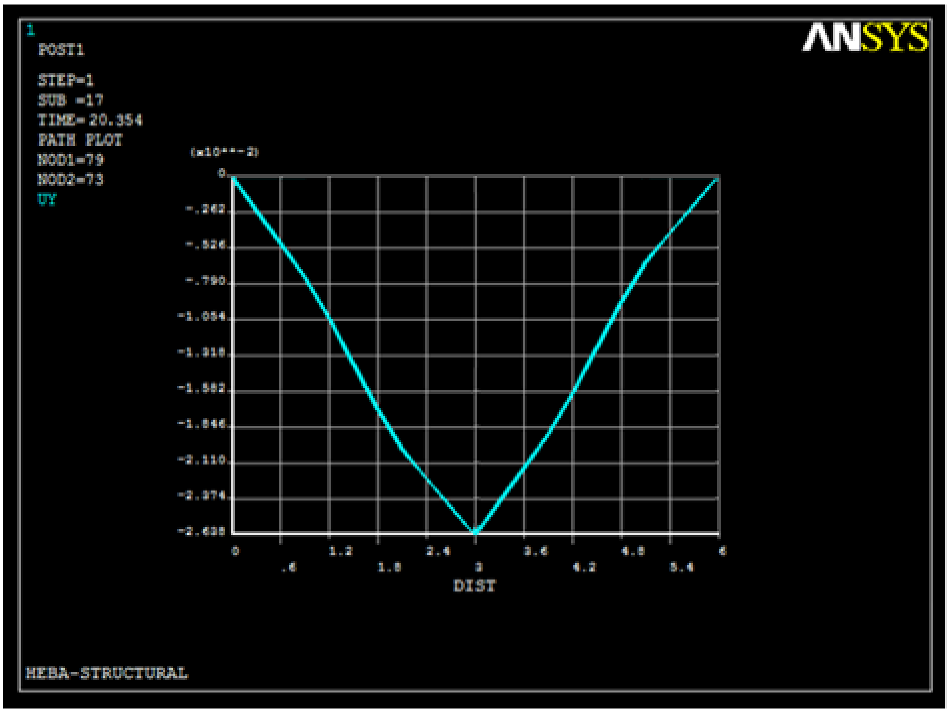

Figure 4.4 Showing the vertical deflection between two support conditions for the beam (RB-SF1) at failure load

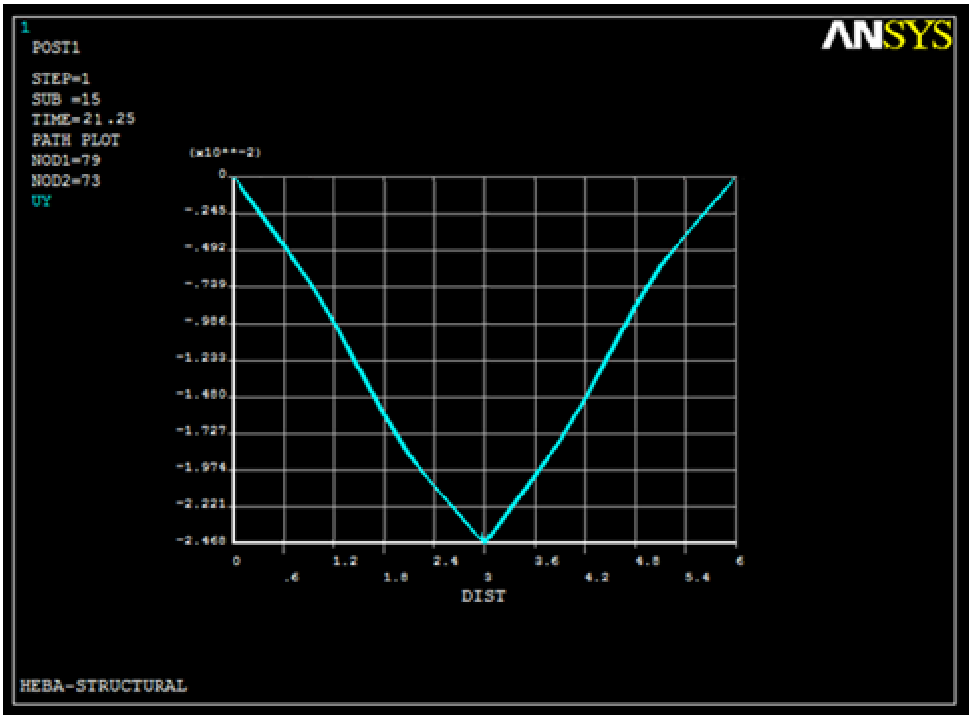

Figure 4.5 Showing the vertical deflection between two support conditions for the beam (RB-SF2.0) at failure load

4.2.4 Pattern of Crack and Mode of Failure

From Figure 4.6, the crack patterns of the tested beam (RB) subjected to point- load at the mid-span of beam up to failure load indicated that the first crack was happened at the bottom face of the beam and near in the maximum bending moment section and when increasing in the applied load, further flexural cracks were featured and expanded vertically upwards in concrete. However, the flexural cracks indicated by small red circles in snapshot from the current ANSYS model and the degree of red color depended on the dimensions (length and width) of crack with less redder denoted to macro crack which especially appeared at the top surface of concrete. Furthermore, at failure load of beam diffusion few cracks progressed in between flexural cracks beside defined as meso cracks (meso cracks indicated by small white circles in snapshot from current ANSYS model) and appeared more cracks form in the shear span including meso cracks, macro cracks and micro cracks (micro cracks indicated by small green circles in snapshot from current ANSYS model).

It was worth to mentioning that the beam failed by crushing of the concrete at the top compression surface was subjected to the point load application.

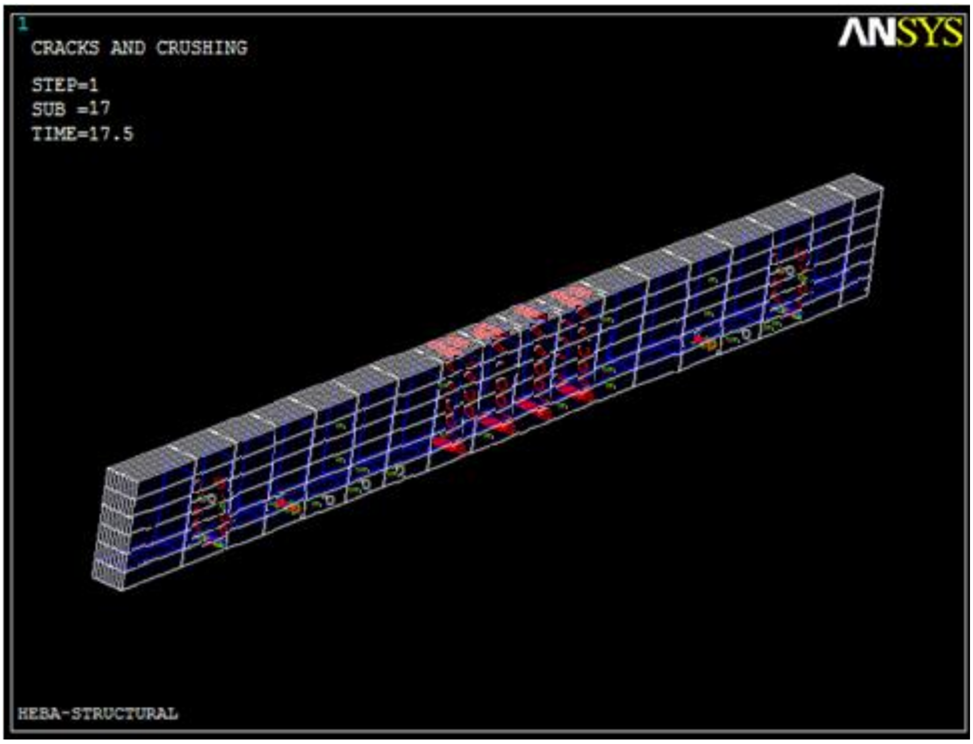

Figure 4.6 Showing the cracks and mode of failure for the beam (RB)

It was clear from Figures 4.7 to 4.10 that increasing the steel fibers content through RC beam were controlled propagation of micro cracks resulted from the steel fibers having large dimensions (diameter and length) relative with those of cracks so that the micro cracks were receded with increasing steel fibers content through the beams RB-SF0.5, RB-SF1.0, and RB-SF2.0, respectively compared with the beam (RB). Moreover, reducing from propagation of the macro cracks through the same beams compared with the beam (RB) due to steel fibers created forces at the level of their lips and transformed gradually to meso cracks when increasing the ratio of volume fraction for steel fibers in soffit of RC beam. It was worth noting that the appearance of flocked or a single incidental crack with randomly propagation were not presented in the beam (RB) (incidental crack indicated by ultrafine blue circles in snapshot from current ANSYS model) which their dimensions were much less than micro cracks and these cracks were relatively increased accompanied by increasing steel fibers content into RC beam.

The appearance of incidental cracks due to the weakness of cohesion between steel fibers and concrete matrix produced by partial interaction phenomenon (no full bonding) was occurred between them. Besides that, grouping incidental cracks were happened resulting from the accumulation of steel fibers in the same location during distributed of them through beam. Notably, all modes of failure were examined on the beams (RB-SF0.5, RB-SF1.0, and RB-SF2.0) also were flexural with crushing of the concrete at the top compression side under the point of load application but least affected for destruction at the top surface of these beams comparative with beam (RB), especially when increased the steel fibers content through RC beam.

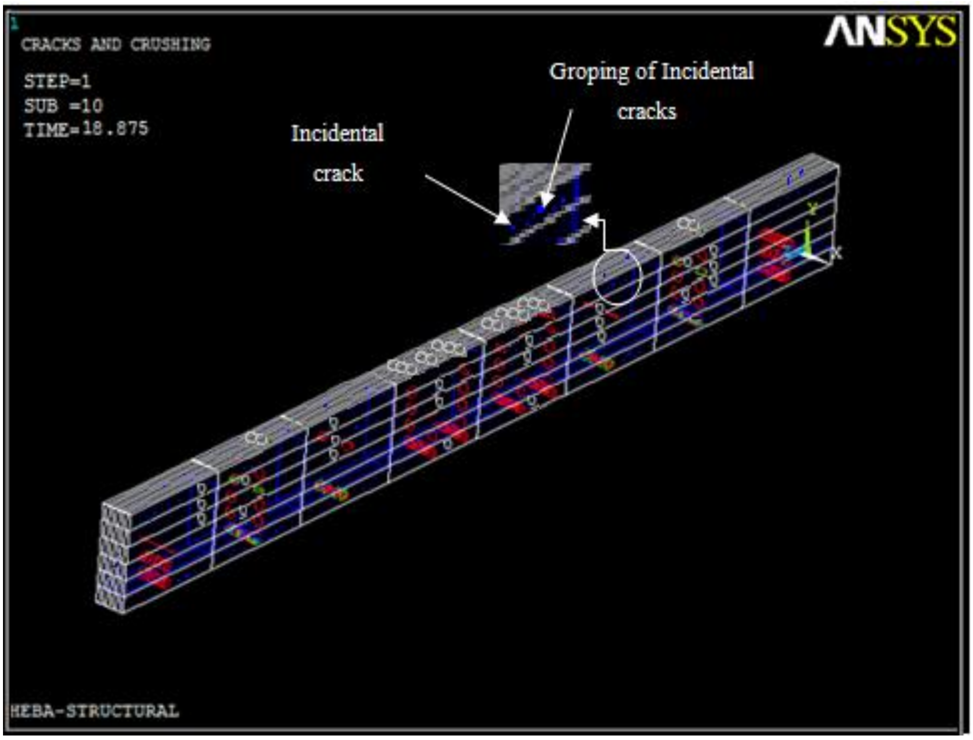

Figure 4.7 Showing the main cracks and distribution of micro-cracks for the beam (RB-SF0.5) at failure load

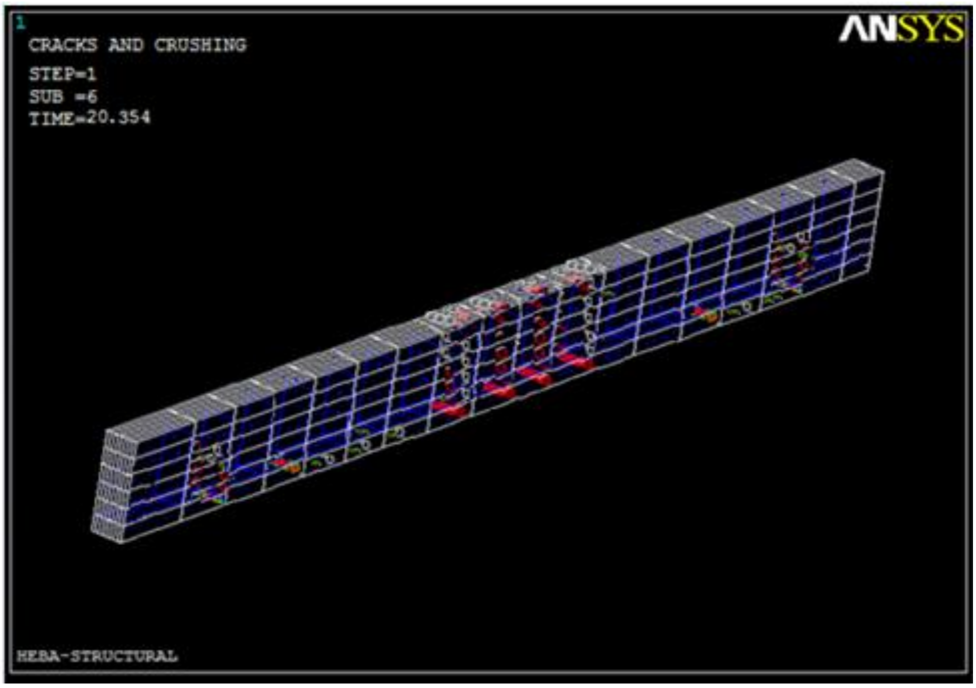

Figure 4.8 Showing the main cracks and distribution of micro-cracks for the beam (RB-SF1.0) at failure load

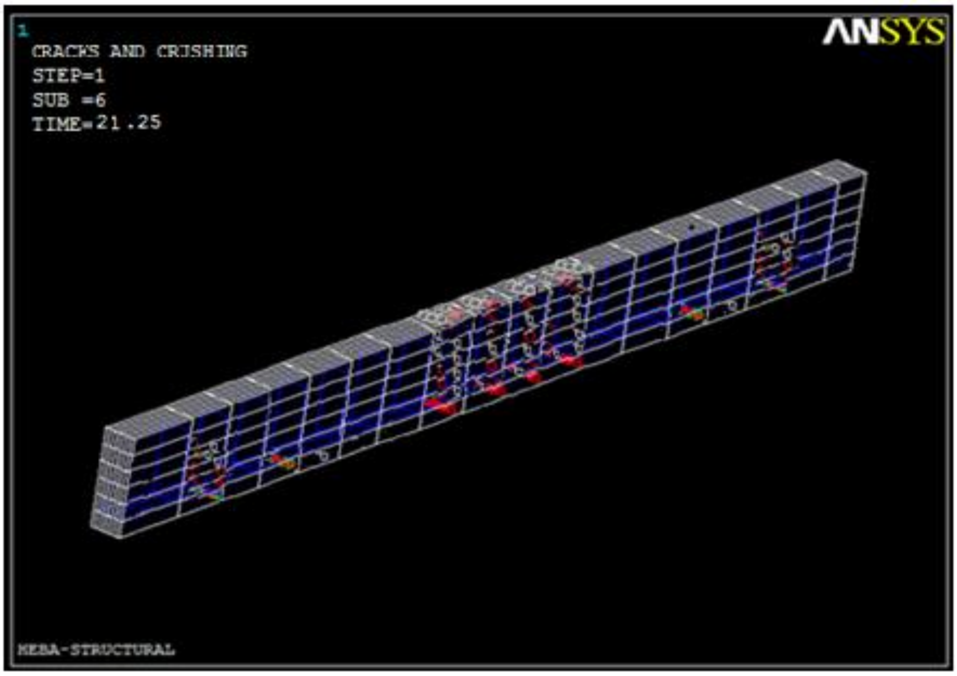

Figure 4.9 Showing the main cracks and distribution of micro-cracks for the beam (RB-SF2.0) at failure load

4.2.5 Validation of ANSYS model with results of previous experimental work for RC beam having steel fibers

In order to validate the results from the current ANSYS model for RC beams strengthened by adding steel fibers, the previous results of the experimental work of Ranjitsinh and Kulkarni (2014) was used. The dimensions and details of the reinforcement for the beam are shown in Figure 4.10. The results obtained from this beam were compared with the results from the current FEM analysis in this part. The comparison was done only for the beams with 0.5 and 1% steel fiber since this reference was used other ratio of volume fraction for steel fibers not be used in the current study which were 0. 25% and 0.75%.

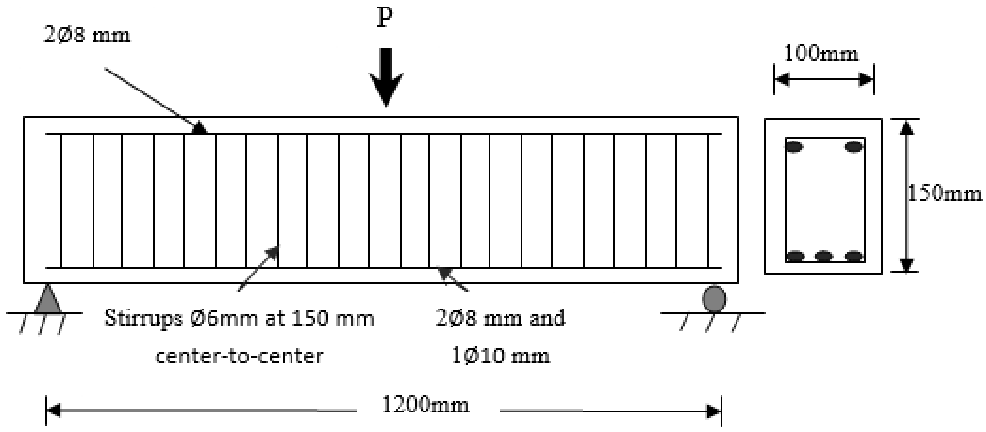

Figure 4.10 Details and dimension of the RC beam tested by Ranjitsinh and Kulkarni (2014)

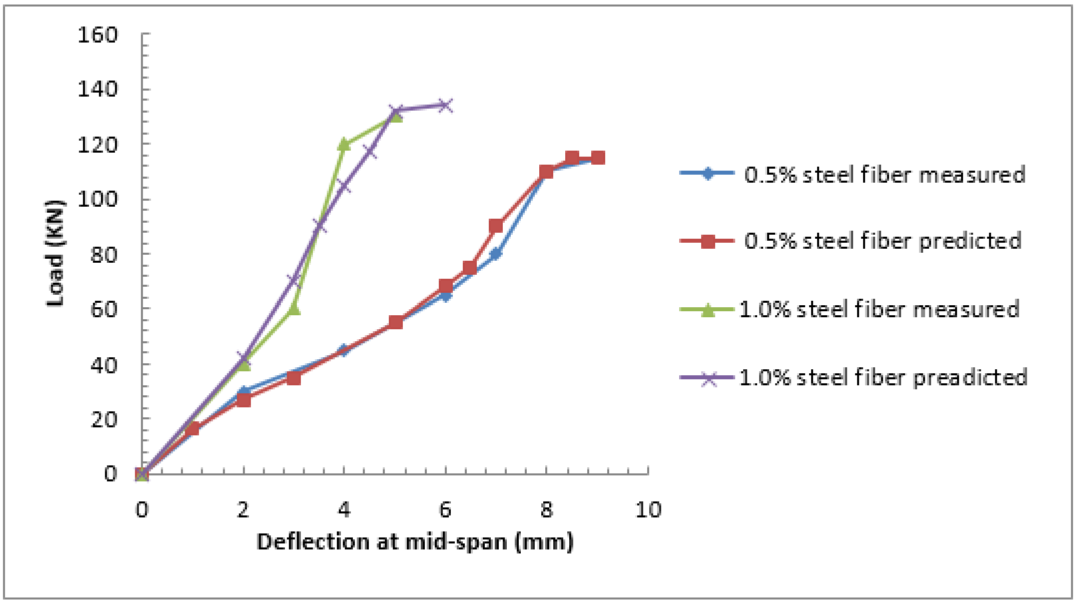

Figure 4.11 Comparison of load-deflection curves for the numerical and experimental results

From Figure 4.11, it could be seen that the maximum difference between current FEM analysis (sparse direct approach) and previous experimental result from Ranjitsinh and Kulkarni (2014) for the beam strengthened by 0.5% steel fibers at loads was within 12.5% when the deflection at 7 mm, while the maximum difference for the beam strengthened by 1% steel fibers at loads was within 11% when the deflection at 5mm. These differences might be attributed to complex behavior of concrete model and neglected the effect of strain hardening of the steel reinforcement in current model.

4.3 Strengthening RC beam by Steel Plates

A technique bonding of steel plate at the lower tension face in RC beam by adhesive resin is required more care representing in ANSYS program due to the friction force and stress concentration generated between them. To model this problem a special surface-to-surface element between these components was used. Moreover, a distinctive element to represent resin adhesive was utilized. The results in terms of deflection, ductility, in addition to crack pattern and mode of failure were given in this part.

4.3.1 Load -deflection relationship

From Figure 4.12 and Table 4.3, it was evident that the increasing of thickness for steel plate at the lower face of RC beam was accompanied by increasing of ultimate failure load. The results of ultimate failure load values at load 20.5 tons, 27.4 tons, and 31.4 tons for beams RB-SP1, RB-SP2, and RB-SP3 respectively, while the ultimate failure load for beam (RB) at load 17.5 tons only. Therefore, to some extent it is concluded that with bonding steel plate at this region responsibility to increase the ultimate tensile strength and increased directly proportional with increasing thickness of steel plate, thus improving the ultimate strength of these beams. Memorable, the maximum percentage delay of appearance ultimate failure was approximately 79.4% for beam (RB-SP3) respect to beam (RB) as shown in Table 4.3.

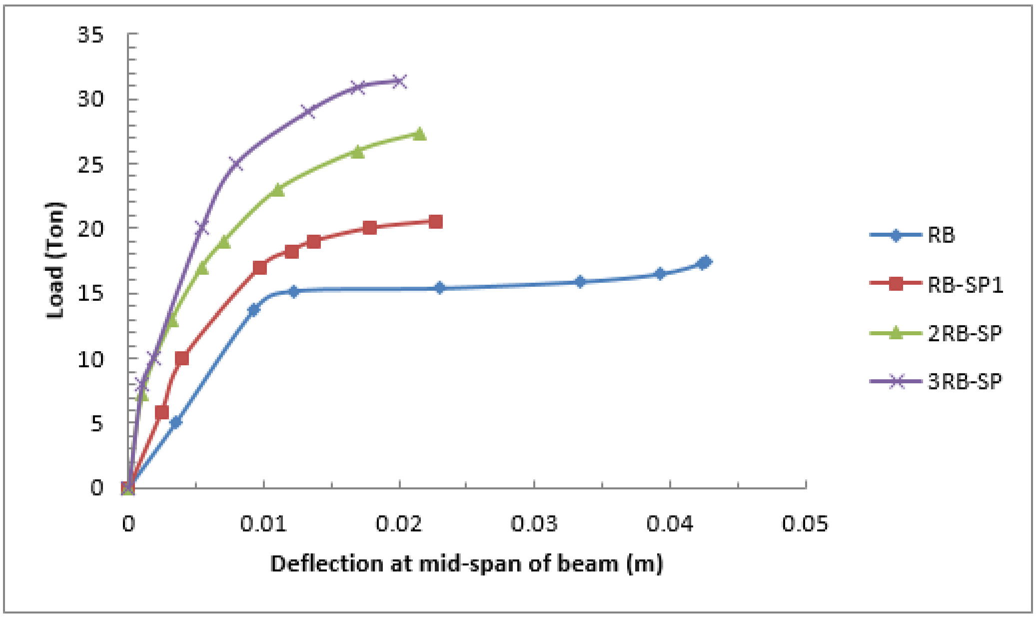

Figure 4.12 Relationship between load-deflection for RC beams with and without steel plate

In addition, Table 4.3 exhibited that the effect of increasing the thickness of steel plate which bonded at the lower tension zone of beam (RB) in delaying the appearance of the first crack value was not significant. The appearance of the first crack for the beams (RB-SP1, RB-SP2, and RB-SP3) were at 4.5 tons, 4.6 tons, and 4.8 tons, respectively, while the appearance of the first crack for the beam (RB) at 4.4 tons since this technique of bonding steel plate made these beams partly more stiffness compared with traditional RC beam.

From Table 4.3, the percentage delay of appearance first cracks for beams (RB-SP1, RB-SP2, and RB-SP3) were 2.3%, 4.5%, and 9.0% respectively, compared with beam (RB). It is worth to mentioning, the first crack was happened at the bottom surface and near the mid-span of these beam.

Table 4.3 The results of the first crack and ultimate failure load for the second group of the beams

Beam	Appearance of First crack at Load (Ton)	Percentage delay of appearance first crack	Failure Load (Ton)	Increment of ultimate failure load (%)
RB	4.4	——	17.5	——
RB-SP1	4.5	2.3	20.5	17.0
RB-SP2	4.6	4.5	27.4	56.6
RB-SP3	4.8	9	31.4	79.4

4.3.2 Ductility

Aforementioned, in part, that by increasing the yield strength of the reinforcement the ductility will decrease and the reported impact of flexural strengthening with external reinforcement decreases the ductility with respect to the reference condition. The results of the current study supported the previous report due to all the strengthened beams by external steel plates (RB-SP1, RB-SP2, and RB-SP3) showed less ductility than that of the reference beam, as shown in Table 4.4.

Table 4.4 Deflection characteristics of RC beams

Beam	Deflection at yield Δ_y (m)	Deflection at Failure Δ_u (m)	Deflection ductility (Δ_u/ Δ_y)	Ratio of deflection ductility
RB	0.0125	0.0426	3.4080	1
RB-SP1	0.0130	0.0240	1.8461	0.54
RB-SP2	0.0142	0.0210	1.4790	0.43
RB-SP3	0.0147	0.0190	1.2930	0.38

From Table 4.4, it was also observed that increasing the thickness of steel plate used for strengthening RC beam at the lower tension face contributed in decreasing the ratio of deflection ductility (Ratio of deflection ductility is the deflection ductility of the strengthened RC beam by bonding a steel plate at the lower tension face (RB-SP1, RB-SP2, and RB-SP3) per the deflection ductility of reference beam (RB)).

4.3.3 Vertical Deflection

The results given in Figures 4.13 to 4.15 showed that the effect of increasing thickness of steel plate whose connected at the maximum tension stress region occurred in RC beam during the loading on the vertical deflection is very important parameter. The beams (RB-SP1, RB-SP2, and RB-SP3) had higher stiffness comparative with the reference beam RB to resist the increasing of loading arising from the increasing steel reinforcement ratio for these beams.

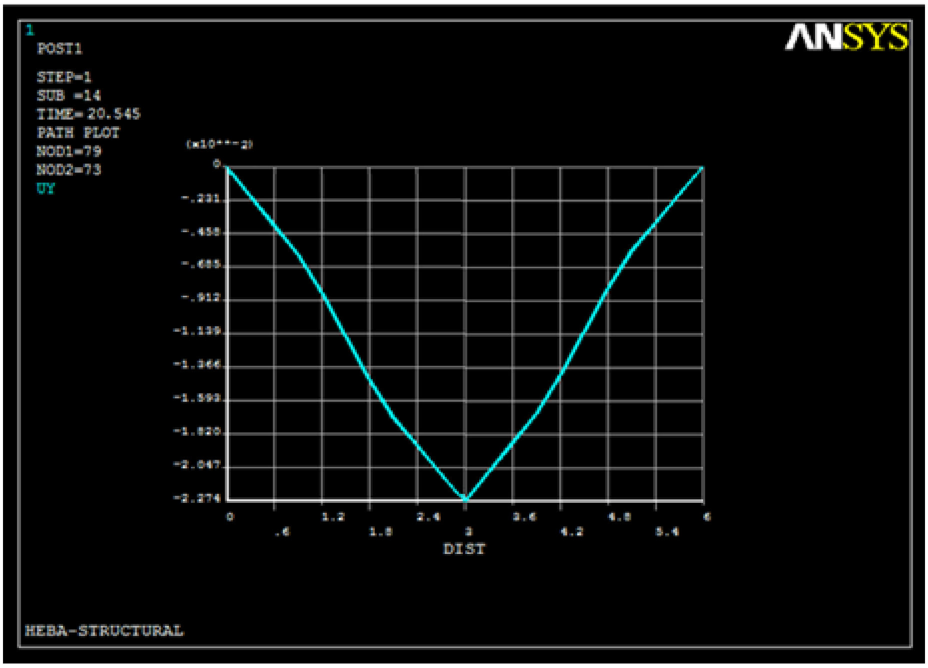

Figure 4.13 Showing the vertical deflection between two support conditions for the beam (RB-SP1) at failure load

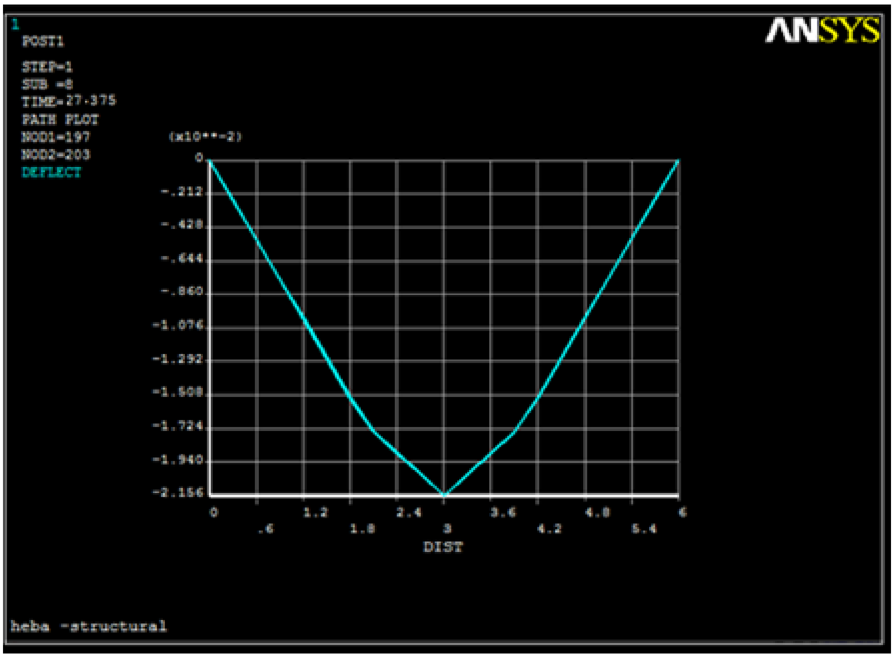

Figure 4.14 Showing the vertical deflection between two support conditions for the beam (RB-SP2) at failure load

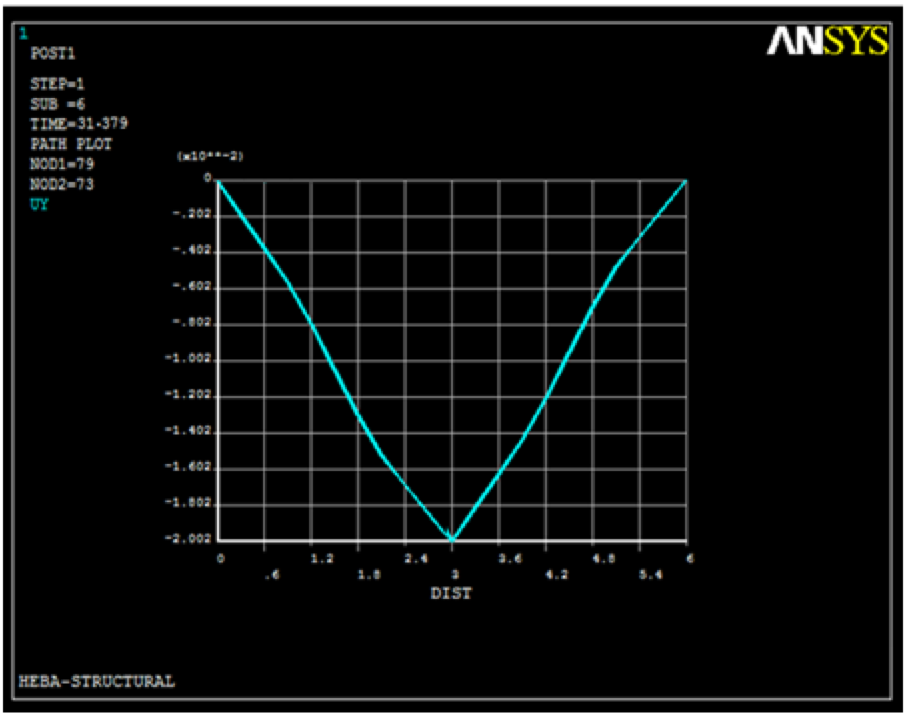

Figure 4.15 Showing the vertical deflection between two support conditions for the beam (RB-SP3) at failure load

4.3.4 Pattern of Crack and Mode of Failure

Figures 4.16 to 4.18 showed the important cracks at the ultimate failure load for the beam RB-SP1, RB-SP2, and RB-SP3, respectively. They were created and propagated at the maximum bending moment zone (flexural cracks). The analysis of the results related that increasing thickness of steel plate which was used for strengthening the RC beam had higher responsibility for increasing the propagation of the flexural cracks at any rate in comparison to the reference beam (RB) from Figure 4.6. Increasing in the flexural crack propagation with increasing the thickness of steel plate resulted in decreasing progressively the flexural strength for these beams. That was also, which it proportional with decreasing in the ductility. On the other hand, from Figures 4.16 to 4.18, at a failure load, the shear cracks and diagonal tension cracks were also gradually increased contributed in increasing thickness of steel plate which was used for strengthening RC beam, especially when thickness of steel plate became 3 mm due to the development of a high stress concentration at the interface surface between steel plate and lower concrete surface triggered by no full composite action between them.

Some cracks were generated in concrete at each end of steel plate which was used for strengthening RC beam and diffused inwards of concrete known as flexural peeling cracks due to steel plate tried to remain straight contrary to concrete when increasing bending moment (curvature) resulted from increasing the applied load. Anyway, the flexural peeling cracks were progressively decreased when increased thickness of steel plate.

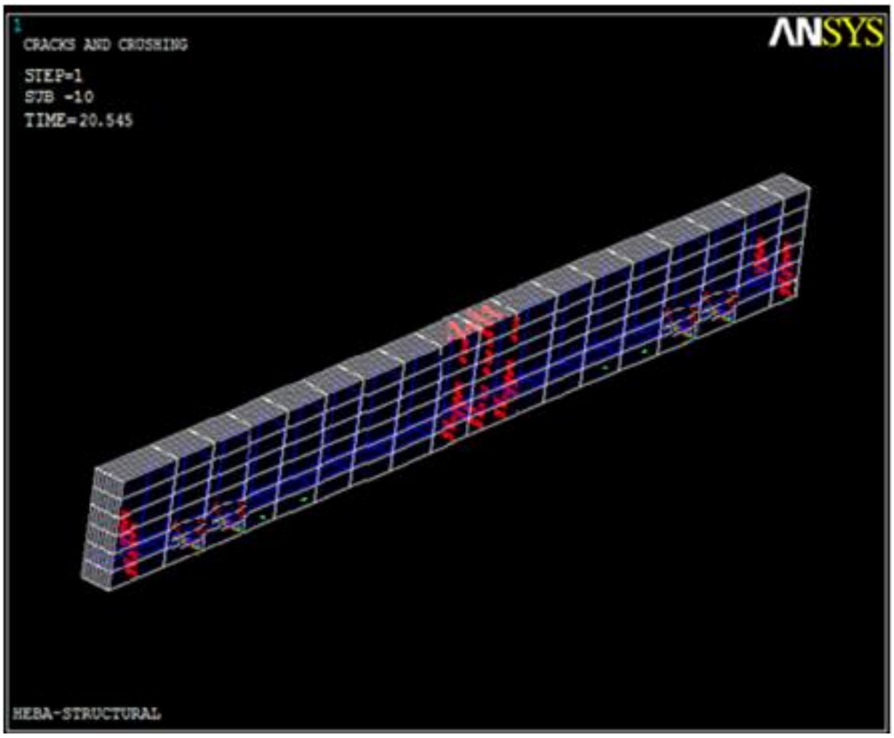

Figure 4.16 Showing the main cracks and distribution of cracks for the beam (RB-SP1) at failure load

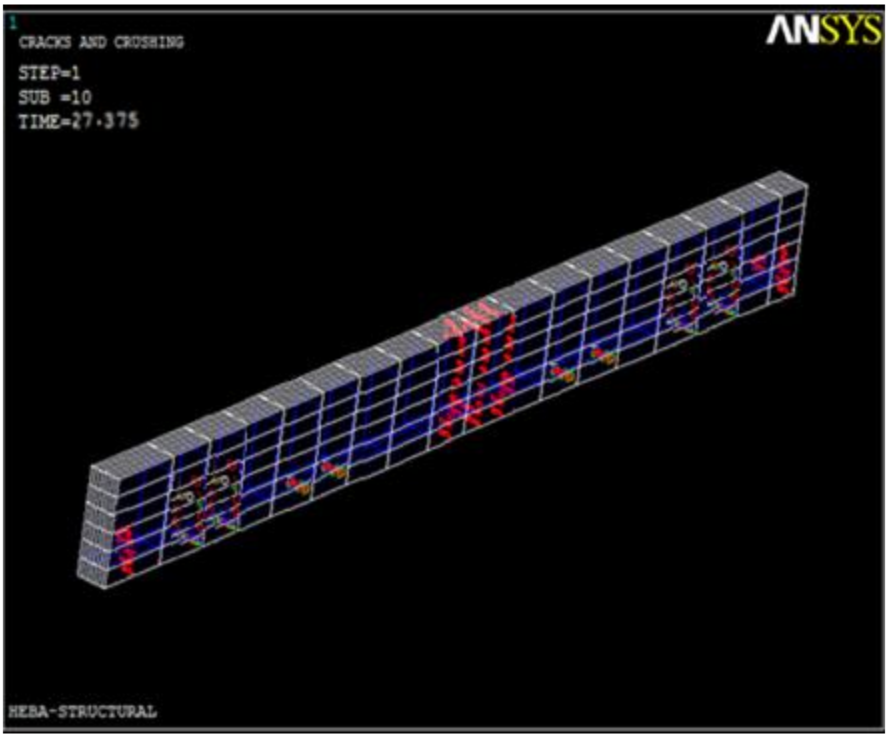

Figure 4.17 Showing the main cracks and distribution of cracks for the beam (RB-SP2) at failure load

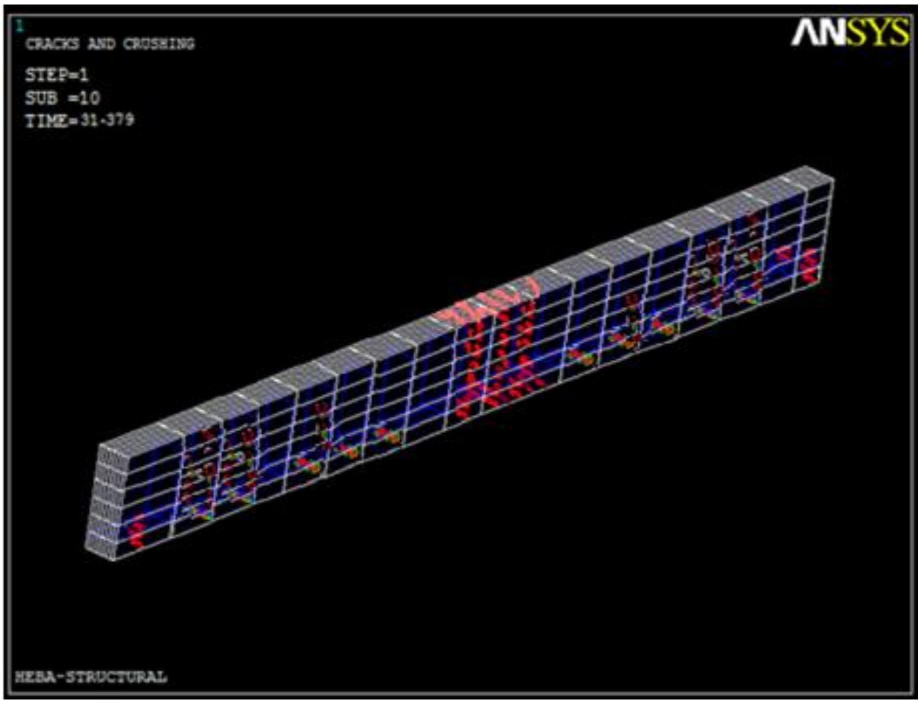

Figure 4.18 Showing the main cracks and distribution of cracks for the beam (RB-SP3) at failure load

4.3.4 Validation of ANSYS model with results of previous experimental work for RC beam with steel plate

The comparison between the results obtained from the current ANSYS model for RC beam strengthened by bonding steel plate at the maximum tension face and results of experimental work by Awadh et al. (2011) was made in this section. The dimension and detail of the test specimen used in this study of Awadh et al. (2011) are given in Figure 4.19. In addition, the accuracy of the FEM model in predicting the experimental results is shown in Figure 4.20.

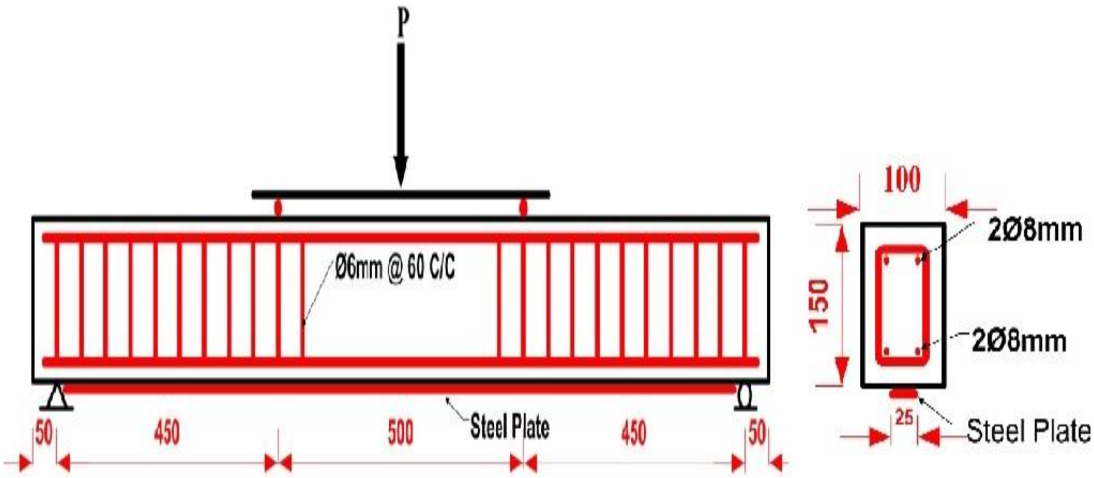

Figure 4.19 Details and dimension of the RC beam in mm tested by Awadh et al. (2011)

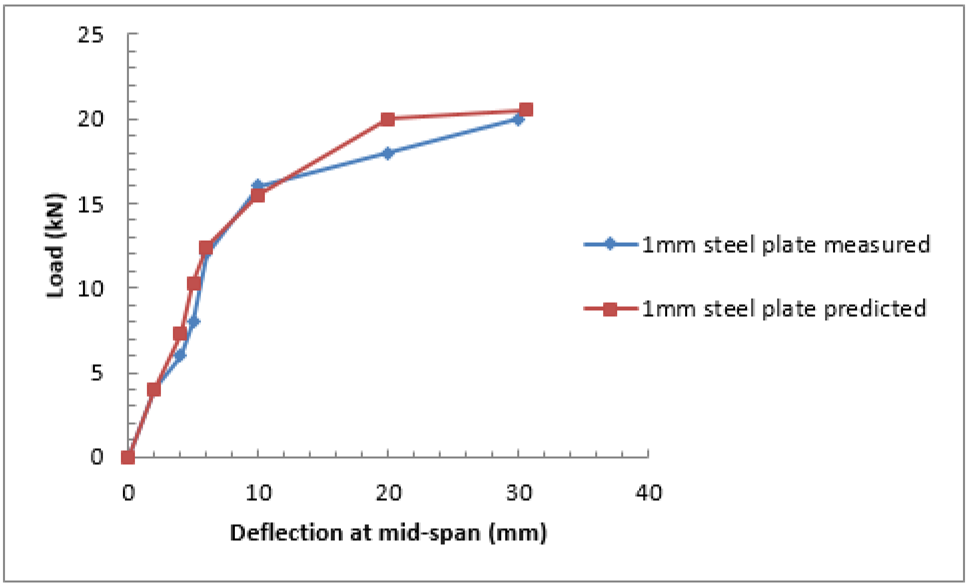

Figure 4.20 Comparison of the load-deflection curves for the numerical and experimental results

From Figure 4.20 it was pointed out that the maximum difference between the results obtained from the current FEM analysis and the experimental results of Awadh et al. (2011) for the beam strengthened by 1 mm steel plate at loads was within 11.1% when the deflection was at 20 mm. Thus, in general, the predicted results matched well with the experimental results. However, small difference was occurred due to the complex behavior of concrete model, beside that ignorant of the effect of strain hardening of the steel reinforcement and the steel plate which it was used for strengthening the beam in current model.

CHAPTER 5

CONCLUSIONS

This study investigated the two strategies of reinforcing RC beams either by using steel fibers in the beam or with bonding steel plate at the lower face. All beams were subjected to concentrated load at mid-span until failure. The finite element method was employed to analyze the structural response of the RC beams. During the analysis, ANSYS software was utilized. Based on the results of this study, the following conclusions can be drawn:

- The retrofitted RC beams by bonding steel plate at the lower face were more effective with regard to ultimate flexural load than the RC beam with the addition of steel fibers. Depending upon the results of load-deflection curve for two strategy of strengthening, at the steel plate with thickness of 3 mm, the increase in ultimate flexural load of the beam was three times more than the flexural strength of the beam with the steel fiber of 2.0% volume fraction.

- From the load-deflection curves, it was also observed that the RC beams strengthening by steel plate had higher stiffness than the RC beam with steel fiber. The maximum vertical deflection was occurred by strengthening RC beam by externally steel plate with thickness 3 mm within 20 mm at failure load 31.4 tons while the maximum vertical deflection was occurred with 2.0% volume fraction of steel fiber at 24.6 mm at load 21.3 tons only.

- Even though the appearance first crack a somewhat delayed in RC beams reinforcing by steel fibers comparable to the RC beams reinforcing by steel plate was not significant.

- In spite of reducing the flexural cracks for RC beams whose strengthening by steel fibers but appearance incidental cracks through beams with irregular distributed might caused by acceleration of failure. In contrast, the RC beams strengthening by externally steel plate which appearance flexural peeling cracks in concrete at each end of plate that used for strengthening but accompanied by diminishing cracks with increasing thickness of steel plate.

- Remarkable increment in the ductility for the RC beams by adding steel fibers was observed 1.35, 1.46 and 1.50, respectively when increased the volume fraction of steel fibers (0.5%, 1.0%, and 2.0%). However, the reduction in the ductility for the retrofitted RC beams with bonding steel plate was 0.54, 0.43 and 0.38, respectively accompanied with increasing thickness (1,2,and 3 mm). Moreover, it was noted to be of steel plate restored the ductility for RC beams strengthened by steel plate when decreased the internal reinforcement.

- All the strengthened beams by steel plate or steel fibers are failed in flexural mode only. Based on the results of this study, increasing percentage of the volume fraction of steel fiber played an essential role in reducing the flexural cracks of the RC beam quite the opposite when increased thickness of steel plate.

- Both strategies of strengthening RC beams significantly increased the capability of absorption energy resulted from increasing the load with time.

REFERENCES

ACI 544. (1978). Measurement of properties of Fiber Reinforced Concrete, *ACI Journal*, pp.283-289.

ACI 544.1. (1996). State-of-the-art report on fiber rein-forced concrete, Farmington Hills, Michigan: American Concrete Institute, pp.1-60.

Agwan, A., August. (1996). Nonlinear Finite Element Analysis of Steel Fiber Reinforced Concrete Members, Mosul University, pp. 237.

Altun, F., Haktanir, T. and Ari, K. (2007). Effects of steel fiber addition on mechanical properties of concrete and RC beams, *Construction and Building Materials*, **21**, pp. 654–661.

Appleton, J. and Silva, V. (1995). Strengthening of reinforced concrete beams by external reinforcement, IABSE Symposium, USA, pp.1178-1184.

Appleton, J. and Gomes, A. (1997). Strengthening Design of Concrete Beams by Addition of Steel Plate, *Engineering Structural*, **41**, pp.15-20.

Aprile, A., Spacone, E., and Limkatanyu, S. (2001). Role of Bond in Beams Strengthened with Steel and FRP Plates, *ASCE Journal of Structural Engineering*, **127**, (12), pp. 1445-1452.

Arslan, Sevuk, F. and Ekiz, I. (2008). Steel plate contribution to load-carrying capacity of retrofitted RC beams, *Construction and Building Materials*, **22**, (3), pp.143-153.

Awadh E., Rana H. and Dina M. (2011). Replacing of Internal Tension Bars by External Bonded Plate, *Journal of Engineering and Development*, **15**, (3), pp.90-103.

Banthia, N. and Trottier, J.F. (1994). Concrete Reinforced with Deformed Steel Fibers, Part I: Bond-Slip Mechanisms, *ACI Materials Journal*, **91**, (5), pp. 435-446.

Banthia, N. (2012). FRC: Milestone in international Research and development, proceedings of FIBCON2012, ICI, Nagpur, India, pp.48.

Brown, J. and Atkinson, T. (2012). Introduction to Steel Fiber Reinforced Concrete on Enineering Performance of Concrete, *International Journal of Scientific and Technology Research*, 1, (4).

Calder, A. J. (1979). Exposure Tests on Externally Reinforced Concrete Beam - First Two Years, Supplementary Report 529, Transport and Road Research Laboratory, Crowthorn, U. K.

Calder, A. J. (1988). Exposure Tests on Externally Reinforced Concrete Beam-Performance after Ten Years, Supplementary Report '129, Transport and Road Research Laboratory, Crowthorn, U. K.

Calder, A. J. (1989). Exposure Tests on 3.5 m Externally Reinforced Concrete Beam -the First 8 Years, Supplementary Report 191, Transport and Road Research Laboratory, Crowthorn, U. K.

Campbell, F.C. (2010). Introduction to Composite Materials, ASM International, pp.1-29.

Chen, B. and Liu, J. (2000). Contribution of hybrid fibers on the properties of the control concrete hybrid fibers, *Cement and Concrete Composites*, **22**, (4), pp. 343-351.

Endgington, J., Hannant, D.J. and Williams, R.I. (1974). Steel fiber reinforced concrete, Current paper CP 69/74 Building research establishment Garston Watford.

Gambhir, M.L. (1995). Concrete Technology. 2nd edition. NEW DELHI: Tata Mc Graw-Hill.

Ganesan, N. and Indira, P.V. (2000). Latex Modified SFRC Beam–Column Joints Subjected to Cyclic Loading, *Indian Concrete Journal*, **74**, (7), pp. 416–420.

Ganesan, N., Indira, P.V. and Kumar, S. P. (2006). Ultimate strength of steel fiber reinforced self-compacting concrete flexural elements, *ISET Journal of Earthquake Technology*, **44**, (3), pp. 445–456.

Goosey, M., Roth, M., Kainmuller, T. and Seiz, W. (1999). Epoxy Resins and Their Formulation Plastics for Electronics, Academic Publishers, pp. 103.

Greenough, T. and Nehdi, M. (2008). Shear Behavior of Fiber-Reinforced self consolidating concrete slender beams, *ACI Material Journal*, **105**, (5), PP. 468-477.

Hesham, A. (2010). Effect of compressive strength and reinforcement ratio on strengthened beam with external steel plate, *Al-Qadisiya Journal for Engineering Sciences*, **3**, (2), pp. 71-82.

Hussain, M., Sharif, Alfarabi, Basunbul, I.A., Baluch, M.H. and Al-Sulaimani, G.J. (1995). Flexural Behavior of Precracked Reinforced Concrete Beams Strengthened Externally by Steel Plates, *ACI Structural Journal*, **92**, (1), pp.14-22.

Iioka, Y. and Higai, T. (1976). Experimental Study on Strengthening Methods for Reinforced Concrete Decks Steel Plate Bonding Technique (Part 2), Report of Japan Highway Corporation Laboratory, pp.142-154.

Iioka, Y., Higai, T. and Hosoda, K. (1977). Experimental Study on Strengthening Methods for Reinforced Concrete Decks Steel Plate Bonding Technique (Part 3), Report of Japan Highway Corporation Laboratory, pp.143-151.

Ishitani, T., Higai, T. and Hosoda, K. (1975). Experimental Study on Strengthening Methods for Reinforced Concrete Decks Steel Plate Bonding Technique, Report of Japan Highway Corporation Laboratory, pp.150-157.

James, J. and Beaudoin. (1990). Handbook of Fiber Reinforced Concrete; principles, properties, Development and Applications, Noyes Publications, New Jersey, United State of America, pp.57-63.

James, G.M., and James, K.W. (2005). Reinforced Concrete: Mechanics and Desig, 4^{th} Edition, Prentice Hall, Upper Saddle River, New Jersey.

Jansze, W., Uijl, J.A.D., Walraven, J.C. (1998). Flexural strengthening with externally bionded steel pltes: Design for beam shear and plate anchorage, Challenges for concrete in the next millennium.

Johnston, C.D. (1974). Steel fiber reinforced mortar and concrete, A review of mechanical properties. In fiber reinforced concrete ACI– SP 44 – Detroit.

Jones, R., Swamy, R. N., Bloxham, J. and Bouderbalah, A. (1980). Composite Behavior of Concrete Beams with Epoxy Bonded External Reinforcement, *International Journal of Cement Composites*, **2**, (2), pp. 91–107.

Jones, R., Swamy, R. N. and Charif, A. (1988). Plate Separation and Anchorage of Reinforced Concrete Beams Strengthened by Epoxy-Bonded Steel Plates, *Structural Engineer*, **66**, (5), pp. 85-94.

Jyoti, N., Ajay, G., Devender, Sh., Kapoor, D.R. and Bhupinder, S. (2013). An Experimental Investigation on Structural Performance of Steel Fibre Reinforced Concrete Beam, *International Journal of Engineering and Advanced Technology*, **2**, (6), pp. 301-304.

Kachlakev, D., Miller, T., Yim, S., Chansawat, K. and Potisuk, T. (2001). Finite Element Modelling of Reinforced Concrete Structures Strengthening with FRP Laminates, Special Report SP316, Oregon Department of Transportation, USA.

Kachlakev D. I. (2004). Finite Element Analysis and Model Validation of Shear Deficient Reinforced Concrete Beams Strengthened with GFRP Laminates, California Polytechnic State University.

Kamran, K. (2012). Properties of Concretes Produced by Single and Combined Hooked End Discontinuous Discrete Steel Fibers, Master's Thesis, Eastern Mediterranean University, Turkey.

Lihua, X., Yin, C., Jie, S. and Dongtao, X. (2008). Nonlinear Finite Element Analysis of Steel Fiber Reinforced Concrete Deep Beams, Wuhan University, *Journal of Natural Science*, **13**, (2), pp.201-206.

Lioyd, G.O. and Calder, A.J.J. (1982). The microstructure of epoxy bonded steel-to-concrete joints, TRRL, Transport Research Laboratory, Crowthorne, suppl.rep.705.

Madana, S.K., Kumar, G. R. and Singh, S.P. (2007). Steel Fibers as Replacement of Web Reinforcement for RCC Deep Beams in Shear, *Asian Journal of Civil Engineering*, **3**, (5), pp. 479-489.

Mahendra, R. and Prakash, S. (2010). Strength Appraisal of Artificial Sand as Fine Aggregate in SFRC, *ARPN Journal of Engineering and Applied Sciences*, **5**, (10), pp.34-38.

Maidl, B.R. (1995). Steel Fibre Reinforced Concrete, Ernst and Sohn.

Martins, P.C., Renzende and Guimaräes, K. D. (1996). The Behaviour of RC Beams Strengthened by Glued Plates or Grouted Additional Rebars, Proceedings of Concrete in the Service of Mankind Congress, Concrete Repair, Rehabilitation and Protection, pp. 599-604

Mohammed, A. (2003). Flexural Behavior of Rectangular Fibrous Concrete Slabs Allowing for Membrane Action, Ph.D. Thesis, University of Technology, Baghdad, pp.190.

Naaman, A.E. and Gopalaratnam, V. (1983). Impact properties of steel fiber reinforced concrete in bending, *International Journal of cement composites and light weight concrete*, **5**, (4), pp. 225-233.

Naaman, A. E. and Najm, H. (1991). Bond-Slip Mechanisms of Steel Fibers in Concrete, *ACI Materials Journal*, **88**, (2), pp.135-145.

Nataraja, M. C., Dhang, N and Gupta, A. P (1999). Stress-strain Curves for Steel Fiber Reinforced Concrete in Compression, *Cement and Concrete Composites*, **21**, (5/6), pp. 383-390.

Ohta, M., Aizawa, I., Momota, K. and Nakamura, T. (1971). Experimental Study on Strengthening Using Steel Plate Bonding for Reinforced Concrete Decks, Technique Note of PWRI in Japanese.

Ramakrishnan, V., Brandshaug, T., Coyle, W. V. and Schrader, E. K. (1980). Comparative Evaluation of Concrete Reinforced with Straight Steel Fibers and Fibers with Deformed Ends Glued Together into Bundles, *ACI Journal Proceedings*, **77**, (3), pp 135-143

Rana, A. (2013). Some Studies on Steel Fiber Reinforced Concrete, *International Journal of Emerging Technology and Advanced Engineering*, **3**,(1), pp 120-127.

Ranjitsinh, K. and Kulkarni, D. B. (2014). Comparative Study of Effect of Basalt, Glass and Steel Fiber on Compressive and Flexural Strength of Concrete, *International Journal of Research in Engineering and Technology*, **3**, (6), pp.436-438.

Raoof, M., and Zhang, S. (1997). An Insight into the Structural Behaviour of R.C. Beams with Externally Bonded Plates, Proceedings of the Institution of Civil Engineers, *Structures and Buildings*, **122**, pp. 477-492.

Remigijus, S. and Gediminas, M. (2007). The Influence of Shear Span Ratio on Load Capacity of Fiber Reinforced Concrete Elements with Various Steel Fiber Volumes, *Journal of Civil Engineering and Management*, **8**, (3), pp 209–215.

SAS ANSYS 10.0. (2005). Finite Element Analysis System, SAS IP, Inc., U.S.A.

Saenz, and Luis, P. (1964). Discussion of Equation for the stress-strain curve of concrete, *ACI Journal*, **61**, (9), pp. 1229-1235.

Seema, B. and Jyoti, B. (2013). Improving Shear Capacity of RC Beams Using Epoxy Bonded Continuous Steel Plates, *International Journal of Advanced Technology in Civil Engineering*, **2**, (1), pp.39-44.

Seppo, H. (1996). Action of Glued Steel Plates in Strengthening of Structures, *Rakenteiden Mekaniikka*, **29**, (3), pp. 69-74.

Smith, S.T. and Teng, J.G. (2003). Shear-Bending Interaction in Debonding Failures of FRP-Plated RC Beams, *Advanced Structural Engineering*, **6**, (3), pp.183-199.

Soroushian, P. and Lee, C. D. (1989). Constitutive Modeling of Steel Fiber Reinforced Concrete under Direct Tension and Compression, *International Conference on Recent Developments in Fiber Reinforced Cements and Concrete*, Cardiff (U.K.), Elsevier Applied Science, pp. 363-377.

Soroushian, P., and Bayasi, Z. (1991). Fiber Type Effects on the Performance of Steel Fiber Reinforced Concrete, *ACI Materials Journal*, **88**, (2), pp.129-134.

Sreeja, M.D. (2013). Behaviour of Steel Fibre Reinforced Concrete Beam under Cyclic Loading, *IOSR Journal of Mechanical and Civil Engineering*, **6**, (3), pp.1-4.

Suguna, K., Raghunath, P. N., Thiruvenkatachari, V. and Nagaradjane, V. (2006). 31st Conference on Our World in Concrete and Structures, Singapore.

Swamy, R. N., Jones, R., and Bloxham, J. W. (1987). Structural Behaviour of Reinforced Concrete Beams Strengthened by Epoxy-Bonded Steel Plates, *Structural Engineer*, **65**, (2), pp. 59-68.

Swamy, R. N., Hobbs, B., and Roberts, M. (1995). Structural Behaviour of Externally Bonded Steel Plated RC Beams after Long Term Exposure, *Structural Engineer*, **73**, (16/15), pp. 255-261.

Teng, J.G., Smith, S.T., Yao, J. and Chen, J.F. (2003). Intermediate Crack-induced Debonding in RC beams and slabs, *Construction and Building Material*, **17**, (6), pp.447-462.

Thomas, J. and Ramaswamy, A. (2007). Shear of prestressed concrete beams with steel fibers, *Journal of structures and Buildings*, **160**, (5), PP. 287-293.

Vairagade, Vikrant, S., and Kavita, S. (2012). Introduction to Steel Fiber Reinforced Concrete on Engineering Performance of Concrete, *International Journal of Scientific and Technology Research*, **1**, (4), pp.139-141.

Veera, M. (2012). Flexural behaviour of steel fiber reinforced high strength rice husk ash cement concrete simply supported beams, *International Journal of Civil and Structural Engineering*, **2**, (4), pp.1138-1143.

Vikrant, S., Vairagade, Kavita, S. and Kene. (2012). Introduction to Steel Fiber Reinforced Concrete on Engineering Performance of Concrete, *International Journal of Scientific and Technology Research*, **1**, (4), pp. 139-141.

Willam, K. J., and Warnke, E. P. (1974). Constitutive Model for Triaxial Behaviour of Concrete, Seminar on Concrete Structures Subject to Triaxial Stresses, *International Association of Bridge and Structural Engineering Conference*, Bergamo, Italy, pp. 174.

Wasan, I. and Tayfur, Y. (2013). Flexural Strength of Fibrous Ultra High Performance Reinforced Concrete Beams, *ARPN Journal of Engineering and Applied Sciences*, **8**, (3), pp.200-2014.

Xu, Z., Hao, G. and Li, H.N. (2011). Experimental study of dynamic compressive properties of fiber reinforced concrete material with different fibers, *Materials and Design*, **3**, (1), pp.42-55.

Ziraba, Y.N., Baluch, M.H., Basunbul, I.A., Sharif, A.M., Azad, A.K. and Al-Sulaimani, G.J. (1994). Guidelines Toward the Design of Reinforced Concrete Beams with External Plates, *ACI Structural Journal*, **91**, (6), pp. 639-646.

Zollo, R.F. (1996). Fiber-reinforced Concrete: an Overview after 30 Years of Development, *Cement and Concrete Composite*, **19**, pp.107-122.

APPENDIX

APPENDIX A

A.1 CONSTITUTIVE RELATIONS

With a view to obtain precise analysis, suitable material models are needed. This chapter displays the concrete, fibrous concrete; steel reinforcement bar and steel plate for strengthening beam and for supporting and loading models that are used in this study.

A.1.1 Compressive behavior of concrete

In current analysis was used a principle of uniaxial stress-strain relationship (Saenz and Luis, 1964) for compression behavior of concrete. This relation can be reviewed below:

$$\sigma = \frac{E_c \varepsilon}{1+R_3\left(\frac{\varepsilon}{\varepsilon_\circ}\right)-R_2\left(\frac{\varepsilon}{\varepsilon_\circ}\right)^2+R_1\left(\frac{\varepsilon}{\varepsilon_\circ}\right)^3} \quad \text{(A-1)}$$

Where:

$$R_1 = \frac{R_E\left(R_f-1\right)}{(R_e-1)^2} \quad \text{(A-2)}$$

$$R_2 = 2R_1 - 1 \quad \text{(A-3)}$$

$$R_3 = R_1 + R_E - 2 \quad \text{(A-4)}$$

Which: R_E is the modular ratio ($\frac{E_c}{E_\circ}$), R_f is the stress ratio ($\frac{f_c^{'}}{f_c}$), R_e is the strain ratio ($\frac{\varepsilon_f}{\varepsilon_\circ}$), and $E_\circ$ is the secant modulus ($\frac{f_c^{'}}{\varepsilon_\circ}$).

Where: E_c is the initial tangent modulus, σ is the stress in concrete, $f_c^{'}$ is characteristic compressive strength of concrete, ε_f is the stress in concrete at the maximum strain, $\varepsilon_\circ$ is strain in concrete at the maximum stress, ε_f is the strain in concrete at the compressive failure.

By derivative equation (A-1) respect to strain component can be found the tangent modulus E_t, as shown in formula below:

$$E_t = \frac{d\sigma}{d\varepsilon} = \frac{E_c[1+R_2\left(\frac{\varepsilon}{\varepsilon_\circ}\right)-2R_1\left(\frac{\varepsilon}{\varepsilon_\circ}\right)^3]^2}{[1+R_3\left(\frac{\varepsilon}{\varepsilon_\circ}\right)-R_2\left(\frac{\varepsilon}{\varepsilon_\circ}\right)^2+R_1\left(\frac{\varepsilon}{\varepsilon_\circ}\right)^3]^2} \tag{A-5}$$

At the end of strain –softening –region, the compressive stress initiates to decrease and the equivalent uniaxial tangent modulus converts negative. Therefore, to prevent the numerical difficulties related with a negative tangent modulus, once the ultimate yield stress $f`c$ has been reached, E_t is set to zero and the concrete pursues like perfectly plastic behavior as shown in Figure A1. The plastic behavior is permitted to propagate through a limited strain $\Delta\varepsilon$, at which time the unbalanced stress is released. This methodology proceeds in a stepwise fashion.

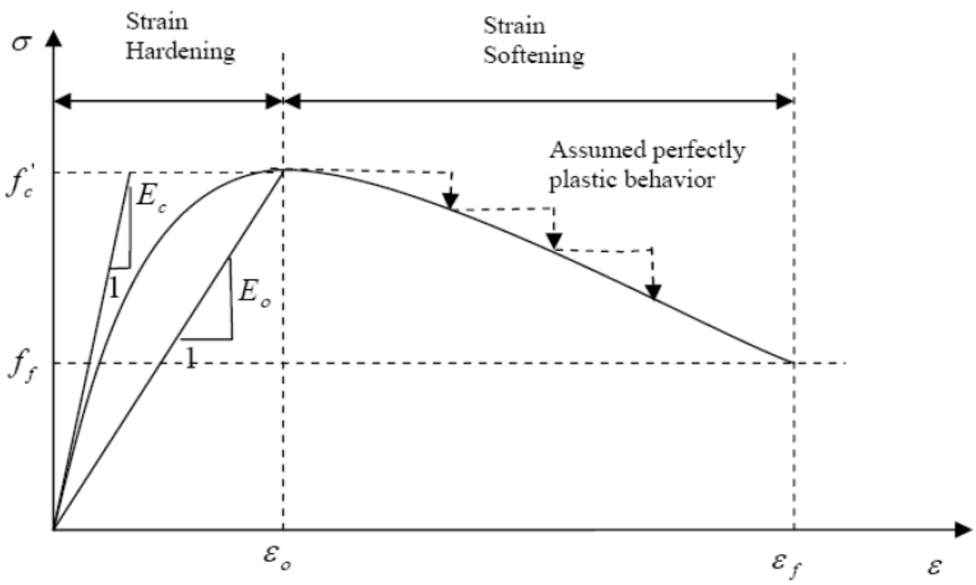

Figure A1 Uniaxial stress-strain curves for concrete (Saenz and Luis, 1964)

A.1.2 Tensile behavior of concrete

Initial tangent modulus *Ec* is used to compute the maximum tensile stress until the macro crack happens in concrete because of these cracks still carry some tensile stress perpendicular to the crack, which is described as tension stiffening. A tension stiffening phenomenon can be shown in Figure A2. The factor of tension stiffening αm was supposed 0.6 in this study. While the tension stiffening stress decreased to zero the default value of the strain ε^* is equal to 0.002. *Et* and *Ec* are the fracture strain to ε^* and modulus of elasticity of tensile concrete between zero to fracture strain, respectively. *f`t* is the maximum stress in concrete at fracture, which has according to strain εt (Saenz and Luis, 1964).

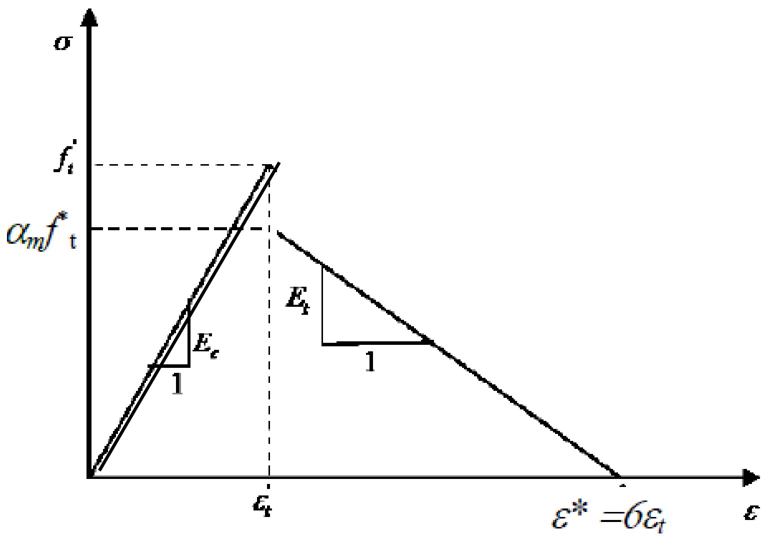

Figure A2 Tension stiffening model

A.1.3 Modeling of Crack and crushing

When the principal tensile stress in any direction locates outside the failure surface cracking in concrete occurs. Crushing happens when all principal stresses were compressive and locate outside the failure surface (William and Warnke, 1974).

Beyond the cracking in concrete, the elastic modulus is set to zero in the direction parallel to the principal tensile stress direction, thereafter; the elastic modulus is set to zero in all directions in case of crushing (SAS, 2005).

A criterion for failure of the concrete under a multiaxial stress state is shown in Figure A3, where σ_{xp} ,σ_{yp} and σ_{zp} are represented the principle stresses in x, y and z directions, respectively. The sign of σ_{zp} is determined the mode of failure (SAS, 2005).

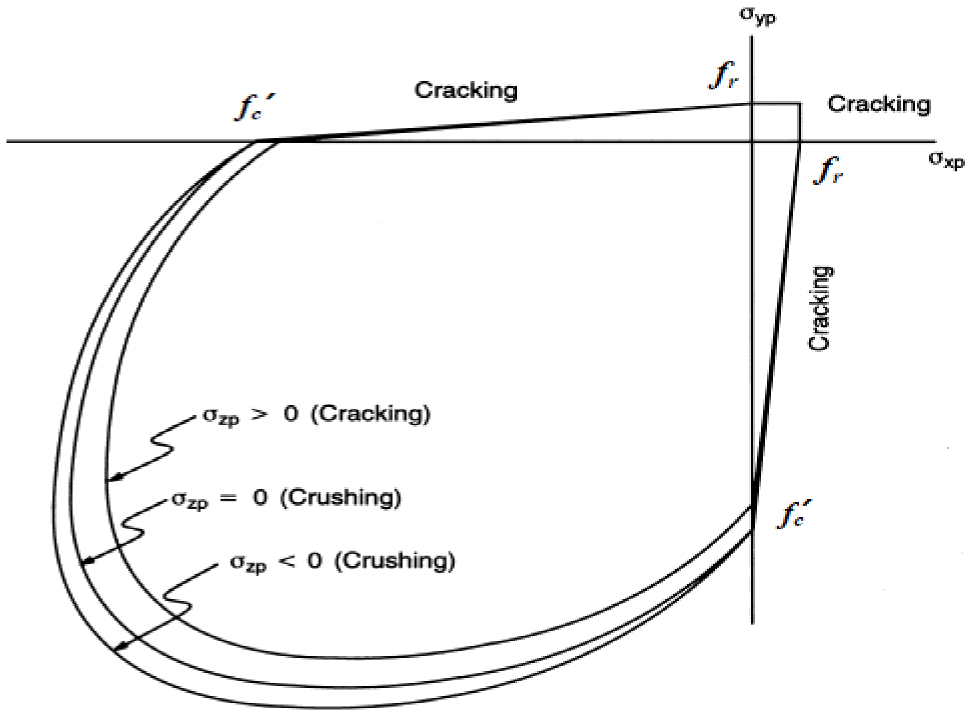

Figure A3 Biaxial failure surface for concrete (SAS, 2005)

A.1.4 Steel reinforcing bars

The stress-strain diagram of the steel reinforcing bar is supposed to be elastic until reaches the steel yield stress (*fy*) then a linear hardening up to the steel ultimate strength (*fu*) as shown in Figure A4. (James et al., 2005).

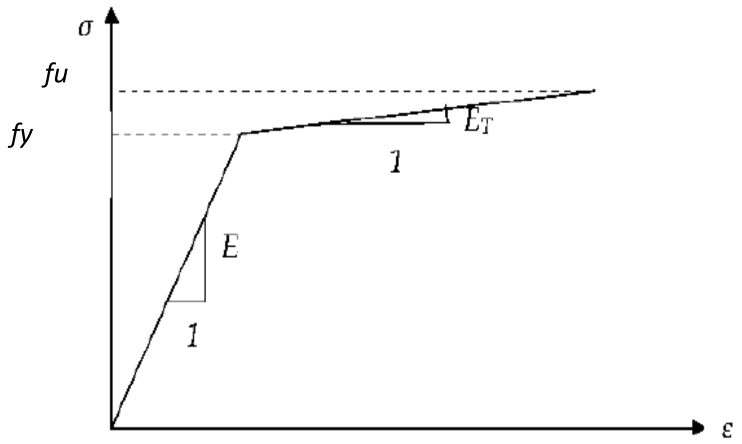

Figure A4 Uniaxial stress-strain relation for steel (James et al., 2005)

A.1.5 Steel plate for strengthening beam

A simple mathematical model is suggested for determining the load- deflection behavior of steel plate reinforcement RC beams. The applied load and boundary condition are shown in Figure A5. The equation for finding deflection(y) between support and load points (Suguna el al., 2006) is given by:

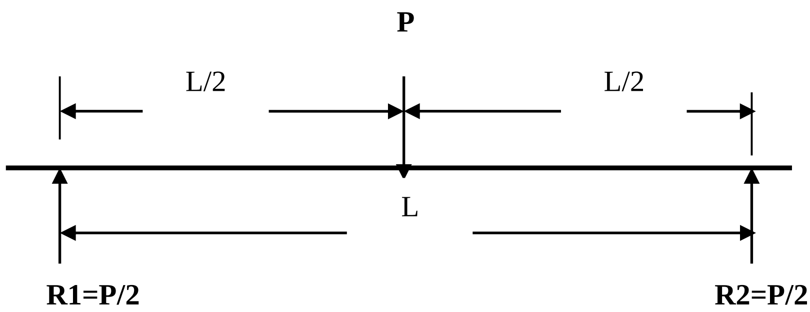

Figure A5 Loading condition under point load at middle span (Suguna el al., 2006)

$$y = \frac{px}{48E_c I_{eff}}[3L^2 - 4x^2] \quad \text{(A-6)}$$

Where:

Ec is the modulus of elasticity of the concrete.

$Ieff$ is the effective second moment of inertia of the section

p is applied load at the mid-span of beam.

x is variable distance begin from side of the beam.

L is length of beam.

The maximum deflection occurs at the mid span of RC beam strengthened by steel plate, at $x = L/2$. Therefore, substituting this value in equation (A-7), we get:

$$y_{max} = \frac{pL^3}{48E_c I_{eff}}$$

(A-7)

The value of I_{eff} is subject to variation over the loading history of steel plate strengthened beam. In the initial stages of loading Concrete, steel rods and steel plate are active in withstanding tensile forces. Concrete cracks in tension region and becomes inactive for tensile resistance in the next stage. This state continues for a considerable fraction of the load history until steel plate yields in tension, closely followed by yielding of internal steel reinforcement. This condition leads to the last stage of the load deflection diagram, where plastic phase of the RC beam leads to large deflections under very small load increments. The effective moment of inertia for initial stage is computed using equations (A-8) and (A-9), respectively. For cracked stage is evaluated using equation (A-10) and (A-11), respectively. Neutral axis transforms up once steel plate and steel rods yield in tension. Extra moments are resisted by increasing the lever arm and not by increase in load. This causes to rapid yielding in compression region, followed by crushing of concrete. Concrete may also crush before steel rods and steel plate reach the yield, in spite of the section may be stronger in tension due to the addition of steel plate.

This way, the strain level in concrete is to be constantly observed over the loading history and failure is said to happen when the strain in extreme fiber of concrete arrives 0.0035.

$$\left[\frac{E_s A_{st}}{E_c} + \frac{E_p A_p}{E_c} + bD\right] n - \left[\frac{bD^2}{2} + \frac{E_s}{E_c} A_{st} d + \frac{E_p}{E_c} A_p \left(D + d_b + \frac{t_p}{2}\right)\right] = 0 \quad \text{(A-8)}$$

$$I_{eff} = \frac{bn^3}{3} + \frac{b(D-n)^3}{3} + \frac{E_s A_{st}(d-n)^2}{E_c} + \frac{E_p A_p\left(D+d_b+\frac{t_p}{2}\right)^2}{E_c} \quad \text{(A-9)}$$

$$\frac{b}{2} n^2 + \left[\frac{E_s A_{st}}{E_c} + \frac{E_p A_p}{E_c}\right] n - \left[\frac{E_s}{E_c} A_{st} d + \frac{E_p}{E_c} A_p \left(D + d_b + \frac{t_p}{2}\right)\right] = 0 \quad \text{(A-10)}$$

$$I_{eff} = \frac{bn^3}{3} + \frac{E_s A_{st}(d-n)^2}{E_c} + \frac{E_p A_p\left(D+d_b+\frac{t_p}{2}\right)^2}{E_c} \quad \text{(A-11)}$$

In the above terms, b is the width of RC beam, d is the effective depth of RC beam, D is the total depth of RC beam, A_{st} is the area of steel rods in tension zone, Ap is the area of steel plate, tp is the thickness of steel plate, db is bond line thickness of adhesive, Es is the modulus of elasticity of steel rods and Ep is the modulus of elasticity of steel plate. Strain in extreme fiber of concrete is considered the prime factor for deciding failure cause of the steel plate strengthened beam. This is assumption is justified since the beam fails by crushing of concrete, whether internal steel reinforcement and steel plate yield or not. For the case of steel rods and steel plate are not yielding, equation (A-10) and (A-11) is enough to evaluate the effective moment of inertia. Contribution of yielded material towards moment of inertia is neglected in the lateral stages.

A.1.6 Design of End Anchorage Length for steel plate

The anchorage length of steel plate that used for strengthening beam is very important parameter must be studied to prevent case premature failure case. However the end anchoring of steel plate is defined the distance between support condition and end of steel plate. In this research, the design of anchorage length of end anchors is suggested depend on the fictitious shear span model by (Jansze et al., 1998). According to this model, steel plate end shear is the governing failure mechanism for end peeling which makes an imaginary shear span on partially bonded with beam as shown in Figure A6. This imaginary shear span can be computed by using the equation (A-12).

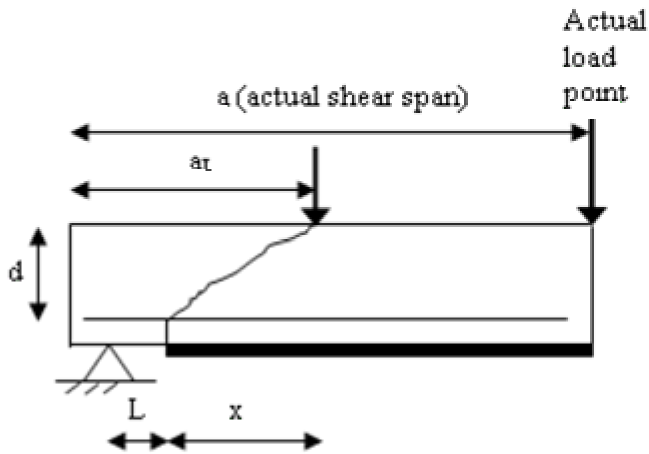

Figure A6 Imaginary shear span (Jansze et al., 1998)

$a_L=[(1-\rho_s)^{0.5})^2 \, dL^3/\rho_s]^{0.25}$ (A-12)

Where:

a_L = imaginary shear span (mm).

ρs = ratio of internal reinforcement (*As/bd*).

d = Effective depth of tension steel bar (mm).

L = Un- plated length of strengthened RC beam (mm).

However, since the shear crack at the end of the steel plate is the main reason which causes the steel plate premature de-bonding, anchors could be progressed along the steel plate portion of imaginary shear span. Therefore, end anchorage length can be obtained by using the equation (A-13) and it should not be more than the effective depth of tension steel bar *(d)*.

Anchorage length;

$x=[a_l-L]\leq d.$ (A-13)

A.1.7 Mechanical Behavior of Fibrous Reinforced Concrete

The combination of steel fiber into concrete improves a large number of its mechanicals properties, especially, when fibers with good mechanical bond were applied. The strain at peak compressive stress ε_{pf} tends to increase because the exits of steel fiber (Soroushian and Lee, 1989):

$$\varepsilon_{pf} = 0.0021 + 0.007\frac{V_f\, l_f}{d_f} \quad \text{(A-14)}$$

Where V_f the volume ratio of steel fiber is, l_f is the length of steel fiber, and d_f denotes diameter of steel fiber V_f .

While, the ultimate strength of fibrous concrete can be computed as the strength of plain concrete known from experiential equation proposed by (Soroushain and Lee, 1989):

$$f_{cf}^{'} = f_{c}^{'} + 3.6\frac{V_f l_f}{d_f} \tag{A-15}$$

Strains at the peak stresses may be computed as was derived by (Agwan, 1996) in micro –strain:

$$\varepsilon_{cuf} = 3011 + 2295V_f \tag{A-16}$$

For fibrous concrete, the modulus of elasticity can be computed (Mohammed, 2003):

$$E_{cf} = E_c\left(1 - V_f\right) + \eta_\circ \eta_1 E_f V_f \tag{A-17}$$

Where: *Ec* and *Ef* are the modulus of elasticity of plain concrete and steel fibers, $\eta_\circ$ is the direction factor and could be taken as 0.41, η_1 is the length factor depends on diameter of fiber, length of fiber and volume fraction.

The product of $\eta_\circ \eta_1$ assumed 0.41 in this study which it is suggested by Palton and Whittaker based on experimental tests achieved to study the stiffness of fibrous concrete (Mohammed, 2003).

The tensile strength $f_{tf}^{'}$ with unit MPa and its corresponding strain ε_{tf} of steel fiber may be computed from (Soroushain and Lee, 1989):

$$f_{tf}^{'} = f_t^{'}\left(1 + 0.016{N_f}^{1/3} + 0.05\pi d_f l_f N_f\right) \quad \text{(A-18)}$$

$$\varepsilon_{tf} = \varepsilon_t\left(1 + 0.35 d_f l_f N_f\right) \quad \text{(A-19)}$$

Where $f`_t$: strength of tensile in concrete (MPa), and N_f: number of steel fibers per unit cross section area and can be computed (Soroushain and Le, 1989):

$$N_f = \eta_{\circ}\left(4V_f/\pi d_f^2\right) \quad \text{(A-20)}$$